

**NASA TECHNICAL
MEMORANDUM**



NASA TM X-3402

NASA TM X-3402

**AN EXPERIMENTAL INVESTIGATION
OF END TREATMENTS FOR
NONRETURN WIND TUNNELS**

*William T. Eckert, Kenneth W. Mort,
and J. E. Piazza*

*Ames Research Center
and U.S. Army Air Mobility R&D Laboratory
Moffett Field, Calif. 94035*



NATIONAL AERONAUTICS AND SPACE ADMINISTRATION • WASHINGTON, D. C. • JUNE 1976

1. Report No. NASA TM X-3402		2. Government Accession No.		3. Recipient's Catalog No.	
4. Title and Subtitle AN EXPERIMENTAL INVESTIGATION OF END TREATMENTS FOR NONRETURN WIND TUNNELS				5. Report Date June 1976	
				6. Performing Organization Code	
7. Author(s) William T. Eckert,* Kenneth W. Mort, and J. E. Piazza*				8. Performing Organization Report No. A-6206	
9. Performing Organization Name and Address NASA Ames Research Center and Ames Directorate, U. S. Army Air Mobility R&D Laboratory Moffett Field, California 94035				10. Work Unit No. 501-06-05	
				11. Contract or Grant No.	
12. Sponsoring Agency Name and Address National Aeronautics and Space Administration, Washington, D.C. 20546 and U. S. Army Air Mobility R&D Laboratory, Moffett Field, California 94035				13. Type of Report and Period Covered Technical Memorandum	
				14. Sponsoring Agency Code	
15. Supplementary Notes *Ames Directorate, U. S. Army Air Mobility R&D Laboratory					
16. Abstract The results of a series of flow quality and performance tests on several inlet and exit configurations for nonreturn wind tunnels are presented. Test section flow angularities, local dynamic pressure variations, and total-pressure-loss variations are presented as functions of wind-to-test-section dynamic pressure ratio. The results show that a nonreturn wind tunnel should have end treatments with three characteristics: (1) a vertical exit system, (2) a horizontal inlet system, and (3) an area of protected enclosure at the inlet. Inlet and exhaust treatments were developed that produced good aerodynamic flow qualities with low power penalties.					
17. Key Words (Suggested by Author(s)) Nonreturn wind tunnels Aircraft testing (V/STOL) Wind protection Wind-tunnel flow quality Wind-tunnel performance				18. Distribution Statement Unlimited STAR Category - 09	
19. Security Classif. (of this report) Unclassified		20. Security Classif. (of this page) Unclassified		21. No. of Pages 57	22. Price* \$4.25

* For sale by the National Technical Information Service, Springfield, Virginia 22161

NOTATION

P_{S_i}	local static pressure at any specific location in the central 75 percent of model test section dimensions (linearly interpolated if not measured), mm of water
P_{S_w}	static pressure of the wind, mm of water
P_{S_0}	average static pressure over central 75 percent of model test section dimensions, mm of water
P_{T_i}	local total pressure at any specific location in the central 75 percent of model test section dimensions (linearly interpolated if not measured), mm of water
P_{T_w}	total pressure of the wind, mm of water
P_{T_0}	average total pressure over central 75 percent of model test section dimensions, mm of water
q_w, Q_w	wind dynamic pressure; $P_{T_w} - P_{S_w}$, mm of water
$\frac{q_w}{q_0}, \frac{Q_w}{Q_0}$	wind-to-test section dynamic pressure ratio
q_0, Q_0	average model test section dynamic pressure taken over the central 75 percent of the test section dimensions; $P_{T_0} - P_{S_0}$, mm of water
R	radius, cm (in.)
V_0	model wind-tunnel test section flow velocity, knots
$\frac{\Delta P}{q_0}, \frac{\Delta P}{Q_0}$	$\left\{ \begin{array}{l} \text{total pressure loss due to friction, rotation, and expansion through model} \\ \text{tunnel circuit because of wind effects; average static pressure rise across the} \\ \text{fans nondimensionalized by test section dynamic pressure (increment from} \\ \text{the no-wind condition)} \end{array} \right.$
$\frac{\Delta P_{T_{\text{circuit}}}}{q_0} \Big _{q_w = 0}$	$\left\{ \begin{array}{l} \text{total pressure loss ratio for the complete model circuit at the no-wind condi-} \\ \text{tion; average static pressure rise across the fans at } q_w = 0, \text{ nondimensional-} \\ \text{ized by test section dynamic pressure} \end{array} \right.$
$\frac{\Delta P_{T_{\text{inlet}}}}{q_0} \Big _{q_w = 0}$	$\left\{ \begin{array}{l} \text{total pressure loss ratio for the inlet system (all components upstream of the} \\ \text{test section) at the no-wind condition; } \frac{P_{T_w} - P_{T_0}}{q_0} \text{ at } q_w = 0 \end{array} \right.$

$\frac{\Delta q}{q_0}, \frac{\Delta Q}{Q_0}$	$\left\{ \begin{array}{l} \text{maximum local dynamic pressure variation for any specific point from the} \\ \text{no-wind condition at the same point, taken over the central 75 percent of} \\ \text{test section dimensions; } \left[\frac{P_{T_i} - P_{S_i}}{q_0} \Big _{q_w \neq 0} - \frac{P_{T_i} - P_{S_i}}{q_0} \Big _{q_w = 0} \right]_{\text{maximum}} \end{array} \right.$
Δu	maximum deviation from the mean axial velocity due to wind effects, taken over the central 75 percent of test section dimensions; $\frac{V_0}{2} \frac{\Delta q}{q_0}$, knots
Δv	maximum deviation from the mean lateral velocity at the centerline due to wind effects (positive to the starboard); $V_0 \tan \theta_s$, knots
Δw	maximum deviation from the mean vertical velocity at the centerline due to wind effects (positive up); $V_0 \tan \theta_u$, knots
θ_s	sideflow angle at the centerline of the model test section, increment from the no-wind condition (positive for air from the port), deg
θ_u	upflow angle at the centerline of the model test section, increment from the no-wind condition (positive up), knots
ψ	azimuth angle of the model centerline with respect to the wind axis (positive for wind from the port), deg

AN EXPERIMENTAL INVESTIGATION OF END TREATMENTS FOR NONRETURN WIND TUNNELS

William T. Eckert,* Kenneth W. Mort, and J. E. Piazza*

Ames Research Center
and
Ames Directorate
U. S. Army Air Mobility R&D Laboratory

SUMMARY

The results of a series of flow quality and performance tests on several inlet and exit configurations for nonreturn wind tunnels are presented. Test section flow angularities, local dynamic pressure variations, and total-pressure-loss variations are presented as functions of wind-to-test-section dynamic pressure ratio. The results show that a nonreturn wind tunnel should have end treatments with three characteristics: (1) a vertical exit system, (2) a horizontal inlet system, and (3) an area of protected enclosure at the inlet. Inlet and exhaust treatments were developed that produced good aerodynamic flow qualities with low power penalties.

INTRODUCTION

In the planning and design of new wind-tunnel facilities the choice between closed- and nonreturn-circuit types is an important one. Possibly offsetting the nonreturn circuit's advantages of continuous fresh test air and lower structural costs is its potential sensitivity to external winds. This sensitivity becomes especially critical at the low test speeds required for V/STOL aircraft studies.

Although many nonreturn wind tunnels have been built (for examples, see refs. 1 through 7), there have been problems either of low operating efficiency or sensitivity to external winds, or both. In the studies described in this report, several combinations and variations of nonreturn wind-tunnel end treatments were examined in an attempt to develop a configuration that had good low-speed flow quality, high efficiency, and minimum structural cost.

Two types of end treatments, vertical and horizontal, were studied for both the inlet and exit ends. The kinds and extent of the treatments were varied, and flow quality and pressure measurements were taken. The flow quality of the tested treatments varied from poor to good; flow quality data of one of the better configurations were compared to the V/STOL flow quality criteria of reference 8.

*Ames Directorate, U. S. Army Air Mobility R&D Laboratory.

MODEL AND APPARATUS

Model

A representative configuration of the model used in this study, installed in the Ames Research Center 40- by 80-Foot Wind Tunnel, is shown in figure 1. Dimensions and geometry of the basic portion of the model tunnel circuit (i.e., without inlet and exit treatment) are given in figure 2 and table 1.

The model was basically a straight, conventional, nonreturn wind tunnel. The primary contractions changed in shape from a rectangular cross section at the entrance to a flat-oval cross section at the test section. (A flat-oval cross section is one with a flat roof and floor and with semicircular sidewalls.) The primary diffuser changed from a flat-oval cross section back to rectangular at the start of the fan section. The fan drive, located near the exit, consisted of eight six-bladed fans, each in a separate nacelle and driven by a small electric motor placed in the center of an annular duct.

Several combinations of inlets and exits were tested. (Figure 3 shows the geometries of the major end treatment components.) The various vertical and horizontal inlet systems (figs. 3(a) through 3(c)) employed such components as perforated plate for roof or walls, protective louvers, square-celled flow straightener grating in several locations, and roof-support posts used as flow guide vanes. The exits (fig. 3(d)) were: (1) a horizontal type with 8-to-1 area ratio (relative to the test section), enclosed with 40-percent-porosity perforated plate on three sides and the roof; (2) an 8-to-1 area ratio vertical exit with small turning vanes; and (3) a 20-to-1 area ratio diffusing vertical exit with large vanes. The detailed geometries of the several inlet/exit combinations are shown in the figures on the pages facing the plots of the data they produced.

Instrumentation

The vertical and transverse locations of the total and static pressure probes and of the flow direction rake in the model test section are shown in figure 4. These pressure probes were located in a plane 6.35 cm (2.5 in.), or 14.7 percent of the test-section length, downstream of the test-section entrance. The static pressure rise across the fans was measured by means of orifices located 0.3 fan diameters ahead of and behind the fan in each nacelle. The pressure data were measured using multiple-tube, water manometers and were recorded photographically.

TEST PROCEDURE

The Ames 40- by 80-Foot Wind Tunnel was used as the source of external wind. The model was mounted on a platform above the boundary layer on the wind-tunnel floor (see fig. 1(b)) and was set at selected azimuth angles to vary the wind direction.

The model test-section dynamic pressure was set at increments between 5.08 and 25.40 cm (2 and 10 in.) of water with the wind dynamic pressure set at values between 0 and 5.08 cm (0 and 2 in.) of water. Both dynamic pressure levels were varied to obtain selected wind-to-test-section

dynamic pressure ratios between 0 and about 1.2. (Within the accuracy of the data, it was found that the results correlated well with this ratio regardless of the absolute value of the dynamic pressures.)

These studies involved only the effects of steady-state winds with a uniform velocity distribution. It was concluded from other studies (refs. 2 and 9) that flow distortion due to the steady-state wind was the most critical problem and that wind gusts produced only a small effect on the turbulence of the test-section flow. Limited studies were performed with the model in a boundary layer artificially thickened to represent the Earth's boundary layer. These tests, not reported here, indicated that a uniform velocity equal to that at the wind-tunnel centerline could be used to establish wind effects on test-section flow quality.

REDUCTION OF DATA

The various parameters were determined in different ways. The test-section dynamic pressure, q_0 , was found from the difference between the average total and average static pressures over the central 75 percent of the test-section vertical and horizontal centerline dimensions. The incremental flow angularity and dynamic pressure variation due to external winds were determined by subtracting the zero-wind values from the wind-on values. The local dynamic pressure variations, $\Delta q/q_0$, were found from linear interpolations of the local total and static pressure data. All data are presented as functions of dynamic pressure ratio, q_w/q_0 .

The azimuth angles for external wind direction were set with an accuracy of about $\pm 1^\circ$. The pressure readings which were used to determine the various flow measurement values were accurate to about ± 1.0 mm (± 0.04 in.) of vertical water column height. The effects of this on the accuracy of the data presented in the figures were determined for the values of model test-section dynamic pressures used in these studies, and are shown in figure 5, for convenience, as functions of the corresponding nominal values of dynamic pressure ratio.

RESULTS

The plotted results of these studies, along with sketches of the 16 configurations, are presented in figures 6 through 21. A configuration plotting index is provided in table 2. In figure 22 the flow quality results from figure 7 are compared with the V/STOL flow quality criteria of reference 8.

DISCUSSION

Inlets

All vertical inlets (figs. 18 through 21) and the horizontal inlet with an open roof (fig. 15) produced very poor flow quality. The wind flow over these inlets produced negative pressure peaks

that caused the serious deficiencies in test-section conditions. Therefore, upward-facing inlets, even if open at the walls as well, should be avoided.

Horizontal inlets without an enclosed area of front protection (figs. 16 and 17) produced results comparable to those for the vertical designs. The need for some front protection area is apparent.

Of those configurations with a horizontal front protection area and a solid roof (figs. 6 through 15), some had better flow quality than others. Similarly, each component of these horizontal inlet systems produced its individual effects. The addition of a flow straightener system at the front of the inlet area, whether completely peripheral or in the central front only, generally served to reduce any test-section flow angularity levels (cf. figs. 10 and 11 with fig. 12). The full peripheral straighteners smoothed the test-section dynamic pressure variations (cf. figs. 10 and 11) but also caused higher sidewall angularities at the higher wind levels. A front flow straightener in combination with roof support posts produced a high dynamic pressure variation at moderate and high wind speeds (fig. 10); the roof posts, when used alone, reduced that variation over the dynamic pressure range (fig. 12).

Exits

Vertical exits appear more desirable than horizontal exits. Generally, the differences in test-section flow quality were small, but the differences in pressure rise across the fans (total circuit losses) were large. For example, consider the horizontal exit data of figure 14 for the case when the wind is from the rear ($\psi = 180^\circ$). These data show a large increase in the total pressure rise across the fans with increasing wind dynamic pressure (increasing Q_w/Q_0). In contrast, the data of figure 11, for a vertical exit, show that a small reduction in pressure rise occurs with increasing wind from the rear. The latter condition is much more desirable since, at a given test-section speed, an increase in total pressure rise requires an increase in power. Similarly, it can be demonstrated that, due to the larger variation in total pressure rise, during gusty conditions when the wind is from the rear, a wind tunnel with a horizontal exit would have more oscillation in test-section speed than would one with a vertical exit. For these two reasons vertical exits appear more desirable than horizontal exits.

Evaluation

Any configuration must be judged against some standard and the V/STOL flow quality criteria of reference 8 are suggested. These criteria are those accepted as standard for conventional wind-tunnel testing ($\Delta\alpha = 0.25^\circ$ and $\Delta u/V_0 = 0.005$) at speeds above 51 m/sec (100 knots), but are modified for speeds between 0 and 51 m/sec (100 knots), since criteria based on freestream velocity lose their significance as the velocity is reduced. At the lower speeds used for testing of V/STOL aircraft, it is recommended that the velocity deviation in each of the three component directions not exceed 0.26 m/sec (0.5 knots).

Figure 22 compares the results of one of the better configurations, that of figure 7, with these suggested V/STOL flow quality criteria. For convenience, the comparisons were made in terms of deviation velocities as functions of test-section velocity at selected wind speeds and directions. In

general the comparisons are favorable, especially at low wind speeds, and particularly in view of the conservative level of the V/STOL flow quality criteria.

Although nearly all of the horizontal inlet configurations produced reasonably acceptable flow quality for low wind conditions (dynamic pressure ratios below about 0.25), none should be considered an optimum design and each could be improved by further careful development work.

CONCLUSIONS

Although no single configuration can be selected best in all respects, this study has developed an end-treatment configuration (fig. 7) that gave good flow quality when coupled with reasonable environmental conditions (i.e., external winds that are not severe). Additional improvements could be obtained by further development of the ideas presented herein.

Though the choice of specific end-treatment components may vary or be subject to appropriate trade-offs between flow quality and cost, three overall conclusions seem clear. A nonreturn wind tunnel designed for good flow quality in the test section and reasonable power efficiency should have (1) a vertical exit, (2) a horizontally facing inlet, and (3) an area of protected enclosure at the inlet.

The merit of an end-treatment system as evaluated against the flow quality criteria will vary depending on prevailing wind direction and speed at the site. Therefore, local wind patterns at the specific wind-tunnel site may alter the suitability of one configuration relative to that of another.

Ames Research Center
National Aeronautics and Space Administration
and
Ames Directorate, U. S. Army Air Mobility R&D Laboratory
Moffett Field, Calif. 94035, February 12, 1976

REFERENCES

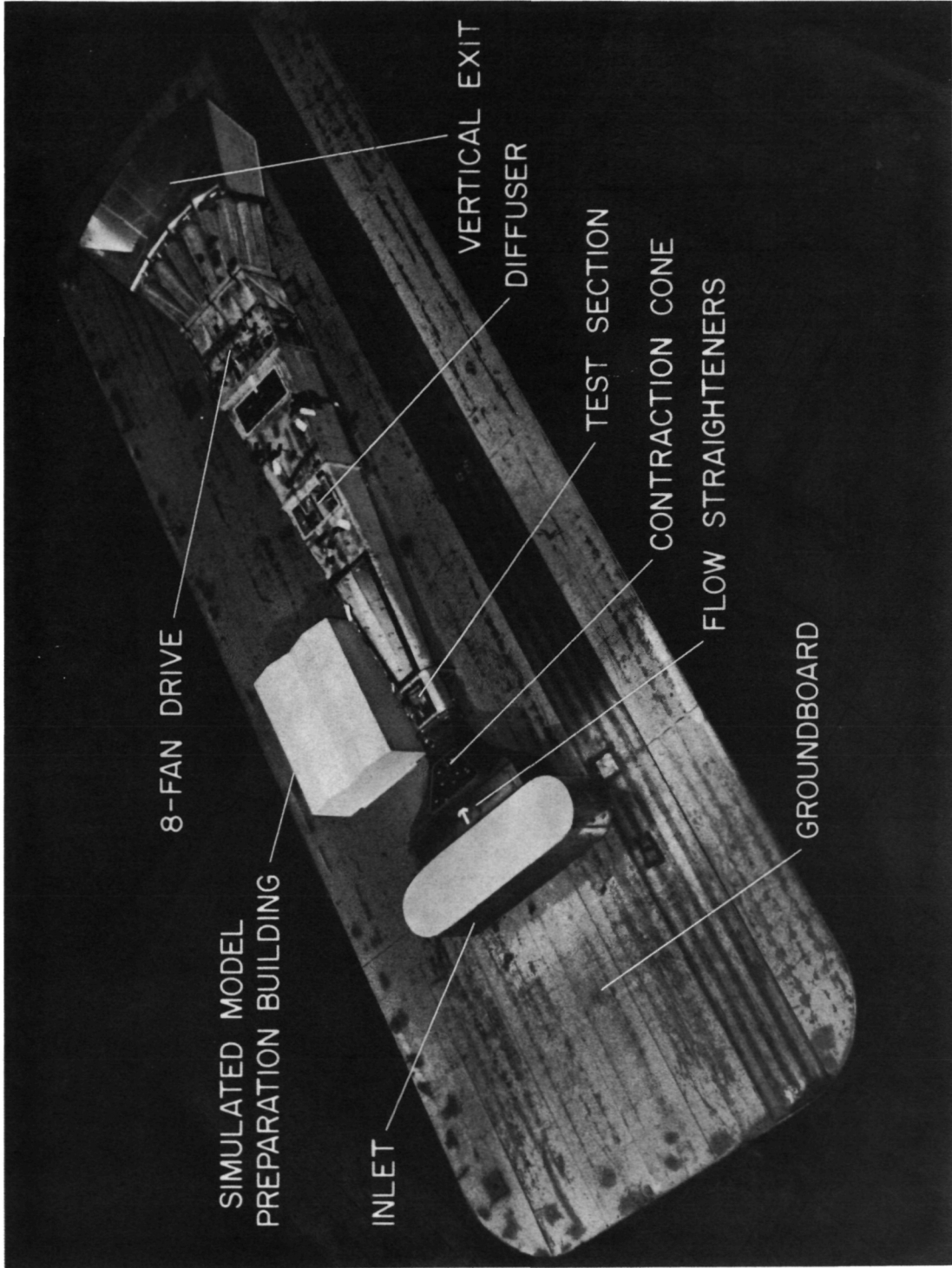
1. Kirk, J. A.: Experience With a V/STOL Tunnel. *J. Roy. Aeronaut. Soc.*, vol. 71, no. 681, Sept. 1967, pp. 606–622.
2. Leef, C. R.; and Hendry, R. G.: Development of a Nonrecirculating Wind-Tunnel Configuration Insensitive to External Winds. *J. Aircraft*, vol. 6, no. 3, May-June, 1969, pp. 221–227.
3. Emslie, K.: Wind Tunnel Tests on Models of V.T.O. Aircraft. AIAA Paper No. 65-720, Nov. 1965.
4. Anderson, C. F.; and Carleton, W. E.: Effects of External Winds on a 1/40-Scale Model of the Open-Circuit Configuration of the Proposed AEDC Multipurpose Low-Speed Wind Tunnel. Arnold Engineering Development Center, AEDC-TR-69-231, Jan. 1970.
5. Wortmann, F. X.; and Althaus, D.: The Laminar Wind Tunnel of the Institute for Aerodynamics and Gasdynamics, Technische Hochschule, Stuttgart, August 1964. Aircraft Research Association, Ltd., Bedford (England). Tr. from *Zeitschrift fur Flugwissenschaften*, vol. 12, no. 4, Apr. 1964.
6. Krishnaswamy, T. N.; Ramachandra, S. M.; and Krishnamoorthy, V.: Design and Characteristics of the 14' × 9' Open Circuit Wind Tunnel. Seminar on Aeronautical Sciences, India, 1961. Proceedings. Bangalore, National Aeronautical Laboratory, 1962, pp. 417–434.
7. Krishnaswamy, T. N.: Selection of the Electric Drive of the 14' × 9' Wind Tunnel. *J. Aeronaut. Soc. India*, vol. 7, no. 2, May 1955, pp. 19–28.
8. Mort, K. W.; Eckert, W. T.; and Kelly, M. W.: The Steady-State Flow Quality of an Open Return Wind Tunnel Model. *Canadian Aeronaut. Space J.*, vol. 18, no. 9, Nov. 1972, pp. 285–289. (Also NASA TM X-62,170, 1972.)
9. Breunlin, Douglas C.; and Sargent, Noel B.: Effect of Transient Winds on the Flow Quality of an Open-Circuit Wind-Tunnel Model. NASA TM X-2538, 1972.

TABLE 1.— MODEL DIMENSIONS

Test section area, m ² (in. ²)	0.083 (128.8)
Flow area at start of fan nacelle contraction, m ² (in. ²)	0.402 (623.0)
Flow area at fans, m ² (in. ²)	0.224 (347.0)
Fan diameter, mm (in.)	213.4 (8.4)
Number of fans	8
Perforated plate (where used)	
Porosity, percent	40
Hole diameter, mm (in.)	3.175 (0.125)
Thickness, mm (in.)	1.016 (0.040)

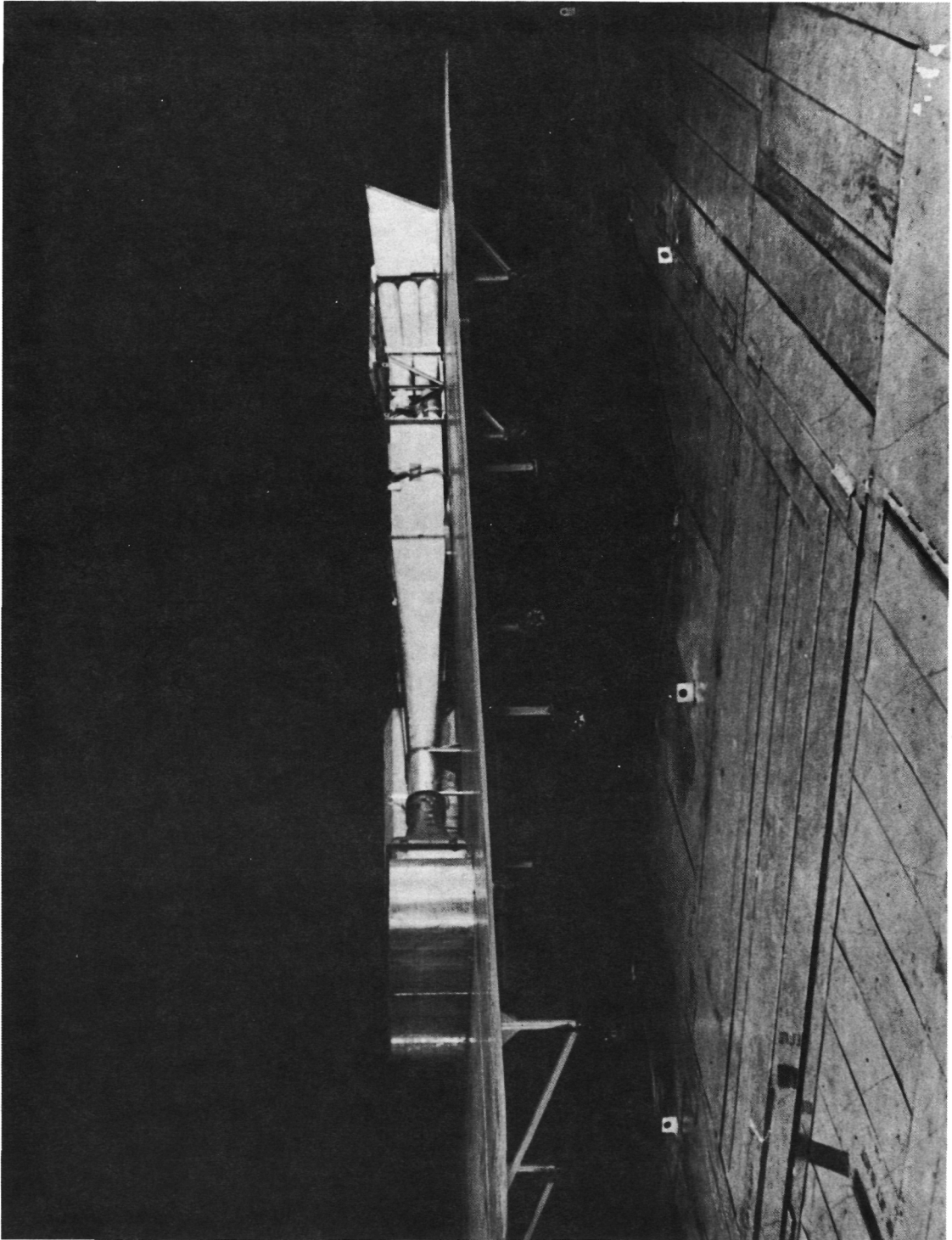
TABLE 2.- SCHEDULE OF CONFIGURATION RESULTS

Figure number	Inlet											Exit	
	Front protection						Comments			Contraction		Type	Description
	Type	Planform size cm x cm (in. x in.)	Roof		Wall type		Flow straighteners		Constant area extension forward of contraction upstream end cm (in.)	Flow straighteners size cm (in.)	Area ratio		
		Type	Supports			Peripheral	Intermediate						
6	Horiz.	58x204 (23x80)	Solid	Posts	40% perf. plate	Front only	Removed		25.4 (10)	2.54x2.54x20.32 (1x1x8)	8	Vert.	Area ratio 20
7						Complete							
8				Removed									
9													Area ratio 8
10		107 x 253 (42x100)		Posts		Front only							Area ratio 20
11						Complete							
12						Removed							Area ratio 8
13						Complete							Area ratio 20
14						Removed							
15						Removed							Horiz. 40% perf. plate
16		89x193 (35 x 76)	40% perf. plate										Vert. Area ratio 8
17		Removed	Removed		Removed			Front louvers	48.26 (19)				
18	Vert.		Grate		Solid			End plate	0	Removed			
19									25.4 (10)	2.54x2.54x20.32 (1x1x8)	8		
20			Solid raised; with grate										
21			None					Vane around inlet					
22	Horiz.	58x204 (23x80)	Solid	Posts	40% perf. plate	Complete		Comparison with criteria					Area ratio 20



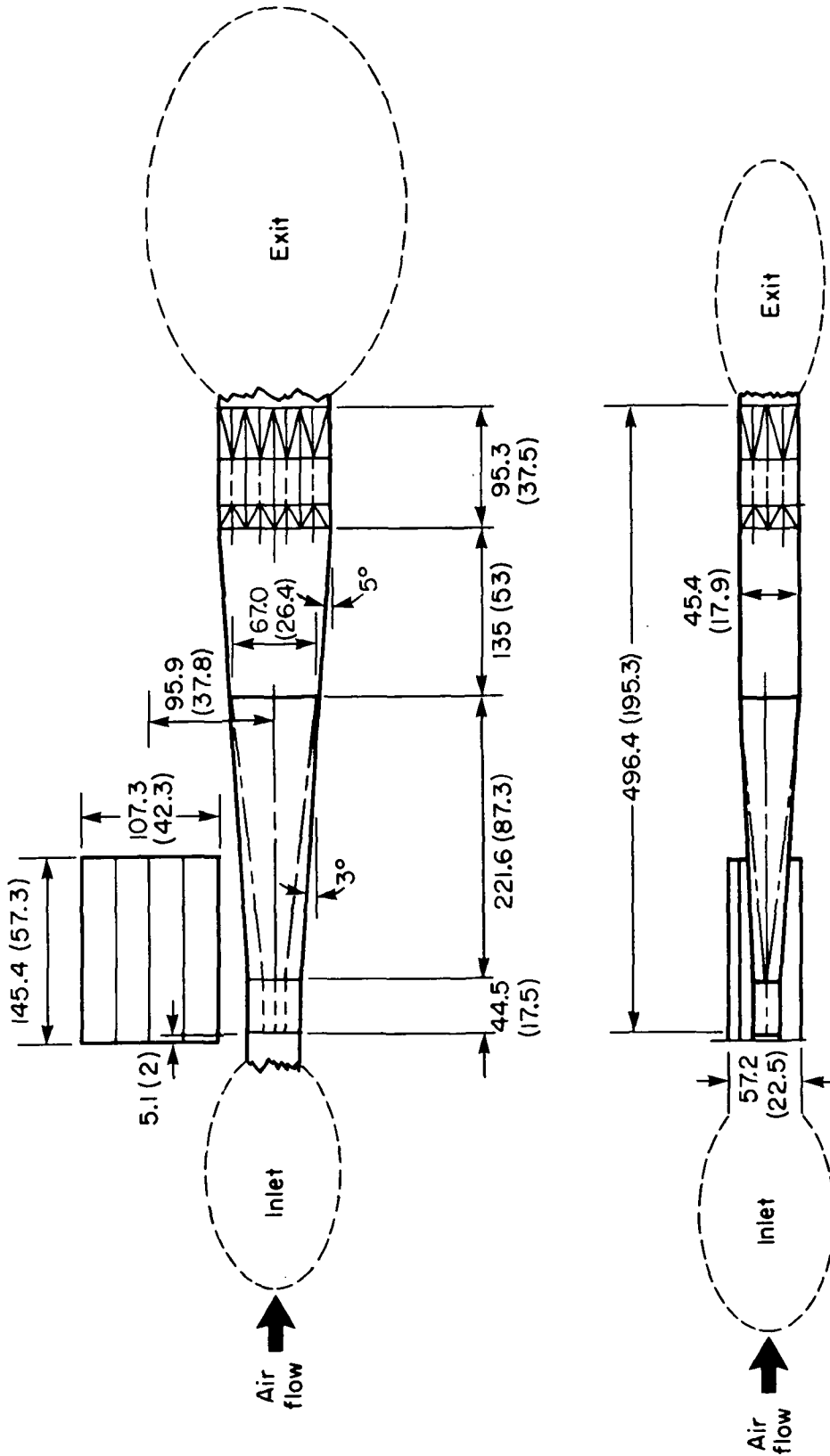
(a) Top view.

Figure 1.- Model with horizontal inlet and vertical exit installed in Ames 40- by 80-Foot Wind Tunnel.



(b) Side view.

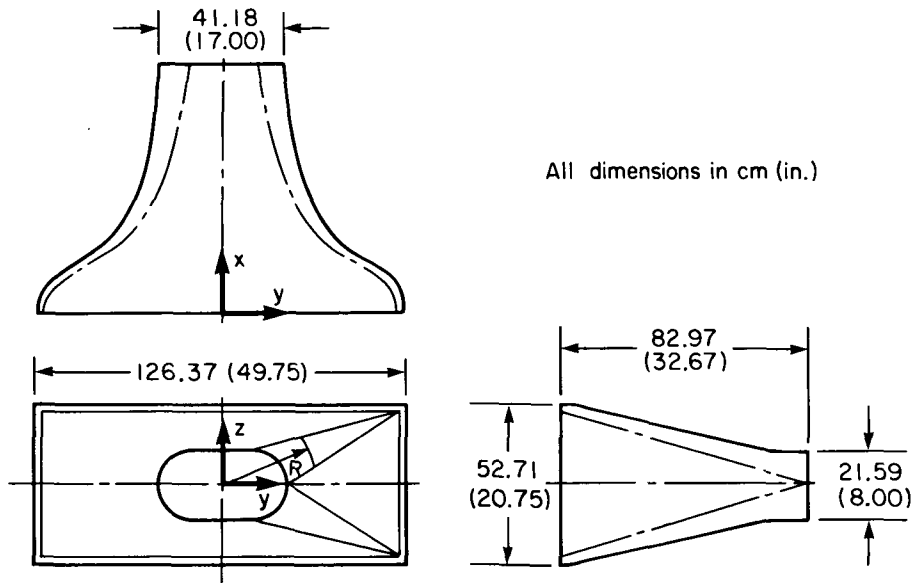
Figure 1.- Concluded.



Dimensions in cm. (in.)
 Inside dimensions shown

(a) Test section, diffuser and fan drive section.

Figure 2.- Geometry of basic model components.

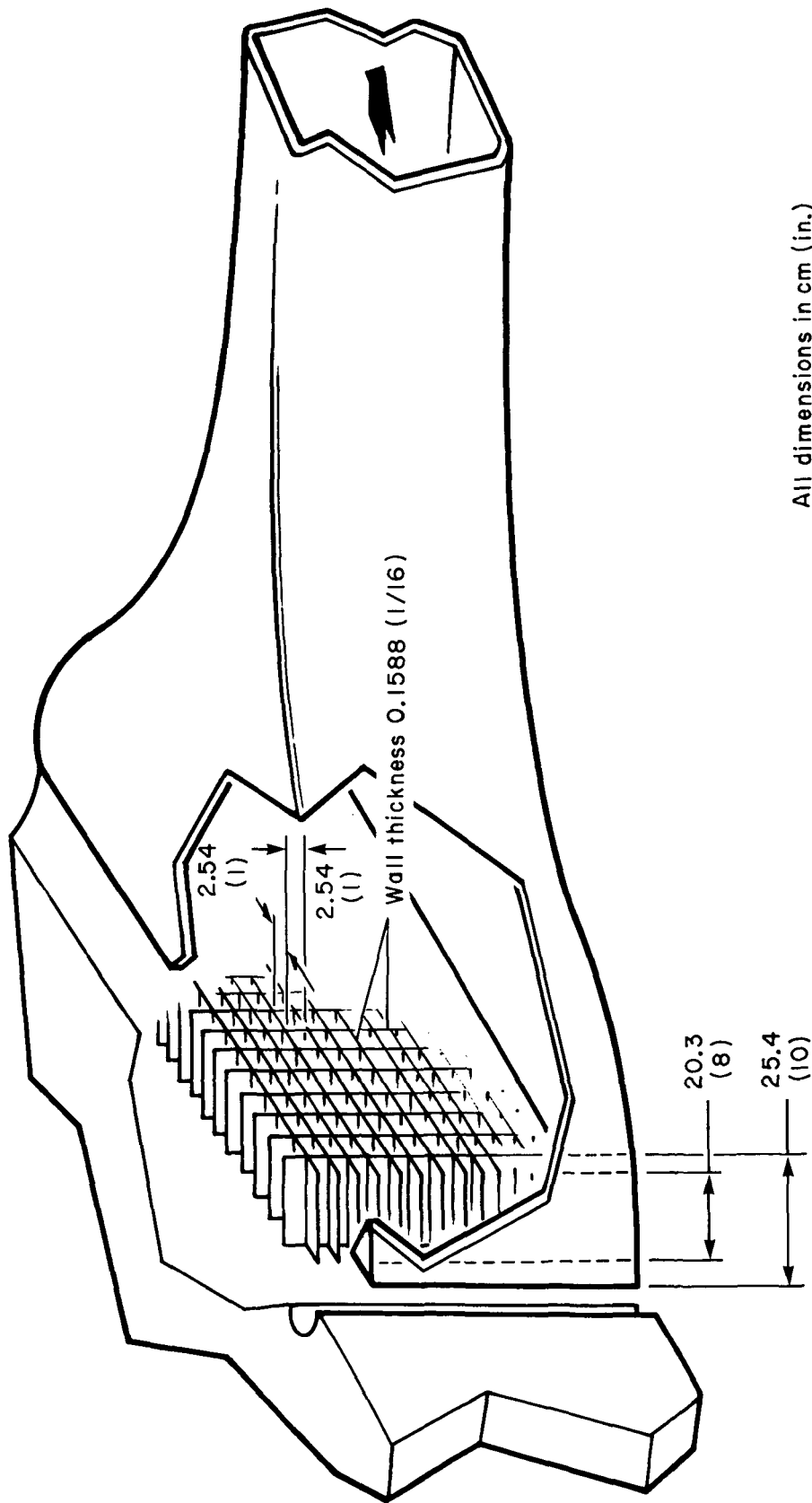


Contraction wall coordinates

X	Y	Z	R
0 (0)	63.20 (24.88)	26.37 (10.38)	0 (0)
2.54 (1)	63.14 (24.86)	26.31 (10.36)	
5.08 (2)	62.84 (24.74)	26.01 (10.24)	1.65 (0.65)
5.33 (2.1)	62.79 (24.72)	25.96 (10.22)	
10.16 (4)	60.43 (23.79)		3.30 (1.30)
13.82 (5.44)	56.24 (22.14)		
15.24 (6)	54.15 (21.32)		4.95 (1.95)
20.32 (8)	47.29 (18.62)		6.60 (2.60)
25.40 (10)	41.48 (16.33)		8.26 (3.25)
30.48 (12)	36.70 (14.45)		9.91 (3.90)
35.56 (14)			10.80 (4.25)
40.64 (16)	29.54 (11.63)		
45.72 (18)			
50.80 (20)	25.10 (9.88)		
54.10 (21.3)	24.10 (9.49)	(13.31) (5.24)	
55.88 (22)			
60.96 (24)	22.71 (8.94)	11.91 (4.69)	
66.04 (26)			
71.12 (28)	21.77 (8.57)	10.97 (4.32)	
76.20 (30)	21.62 (8.51)	10.82 (4.26)	
82.98 (32.67)	21.59 (8.50)	10.80 (4.25)	10.80 (4.25)

(b) 8:1 contraction cone A.

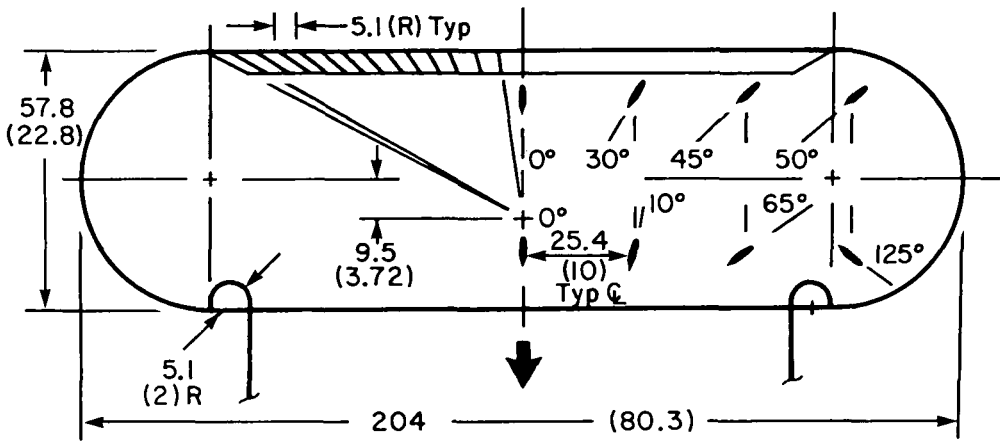
Figure 2.- Continued.



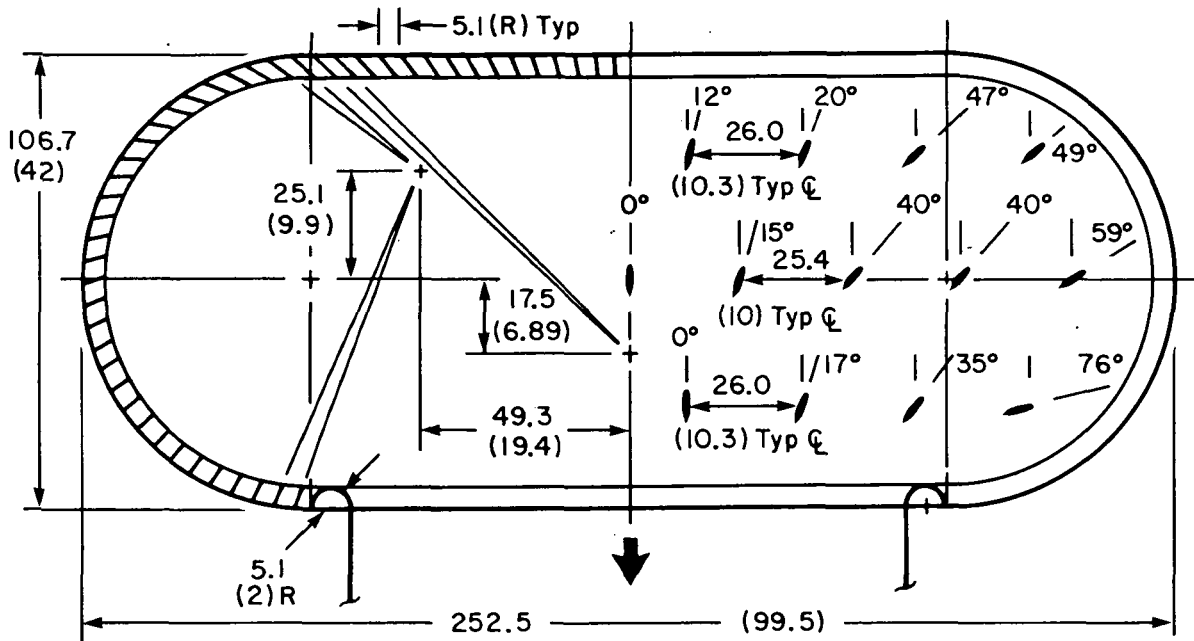
All dimensions in cm (in.)

(a) Contraction flow straighteners at entrance to contraction cone.

Figure 3.- Geometry details of major end treatment components.

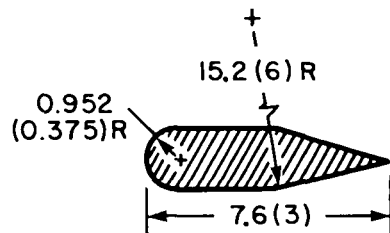


Small inlet — 58 × 204 cm (23 × 80 in.)
(With front flow straightener)



Large inlet — 107 × 253 cm (42 × 100 in.)
(With peripheral flow straightener)

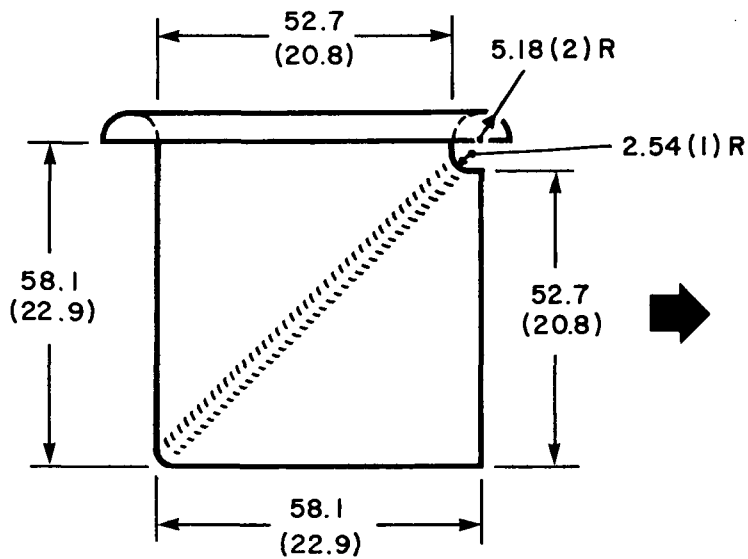
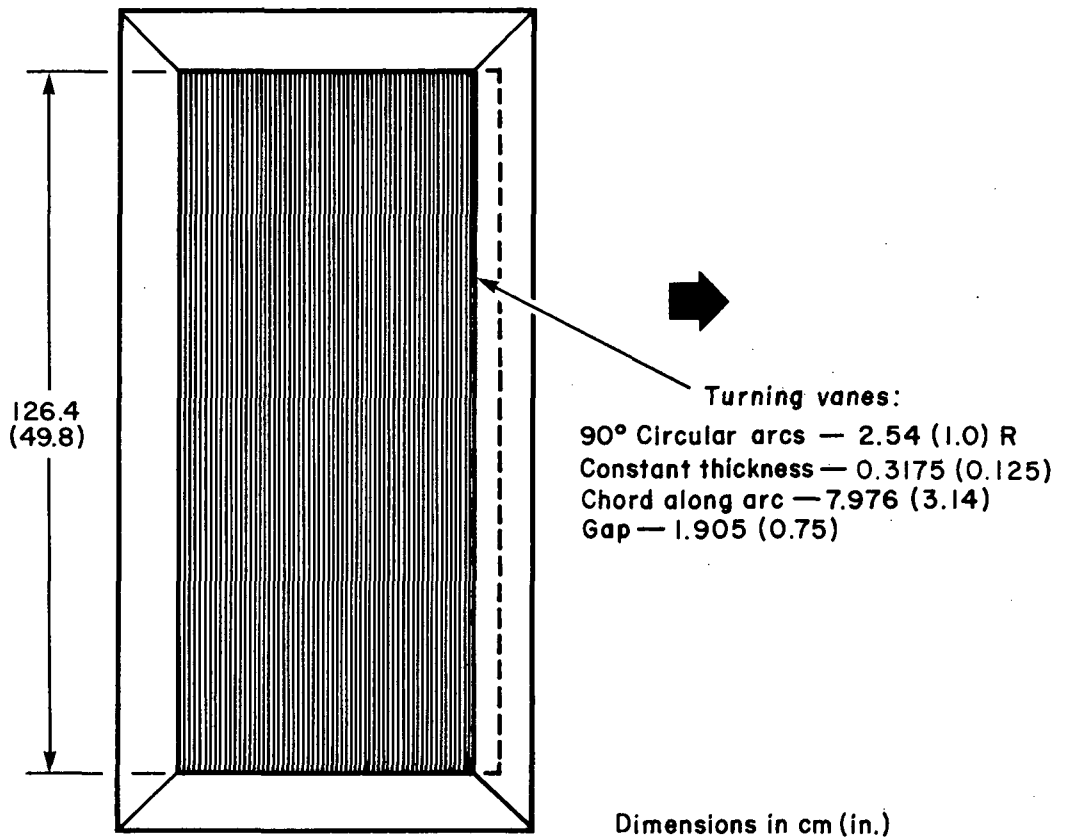
Dimensions in cm (in.)
Geometry symmetrical about longitudinal centerline



Roof post cross section

(b) Horizontal inlet area planform and post arrangement details.

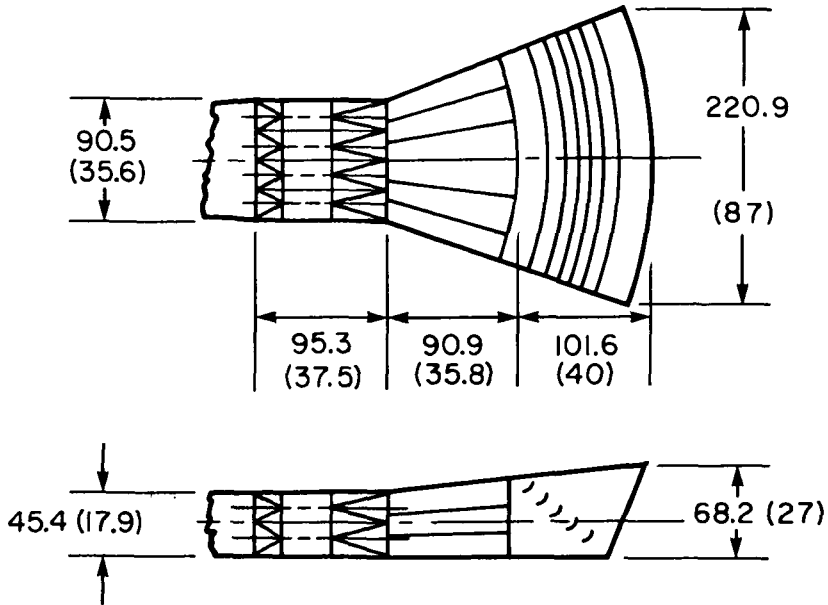
Figure 3.- Continued.



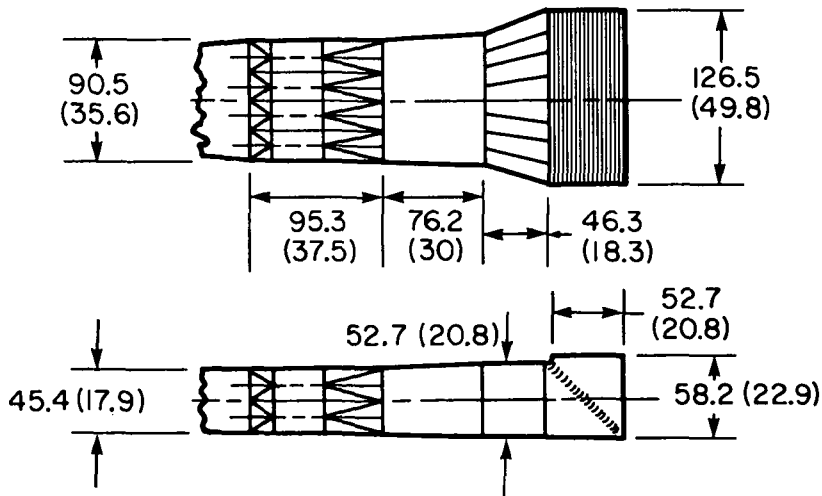
(c) Basic area ratio 8:1 vertical inlet.

Figure 3.- Continued.

All dimensions in cm (in.)



Area ratio 20:1 (Basic) Vertical exit



Area ratio 8:1 (Alternate) Vertical exit

(d) Exit configurations.

Figure 3.- Concluded.

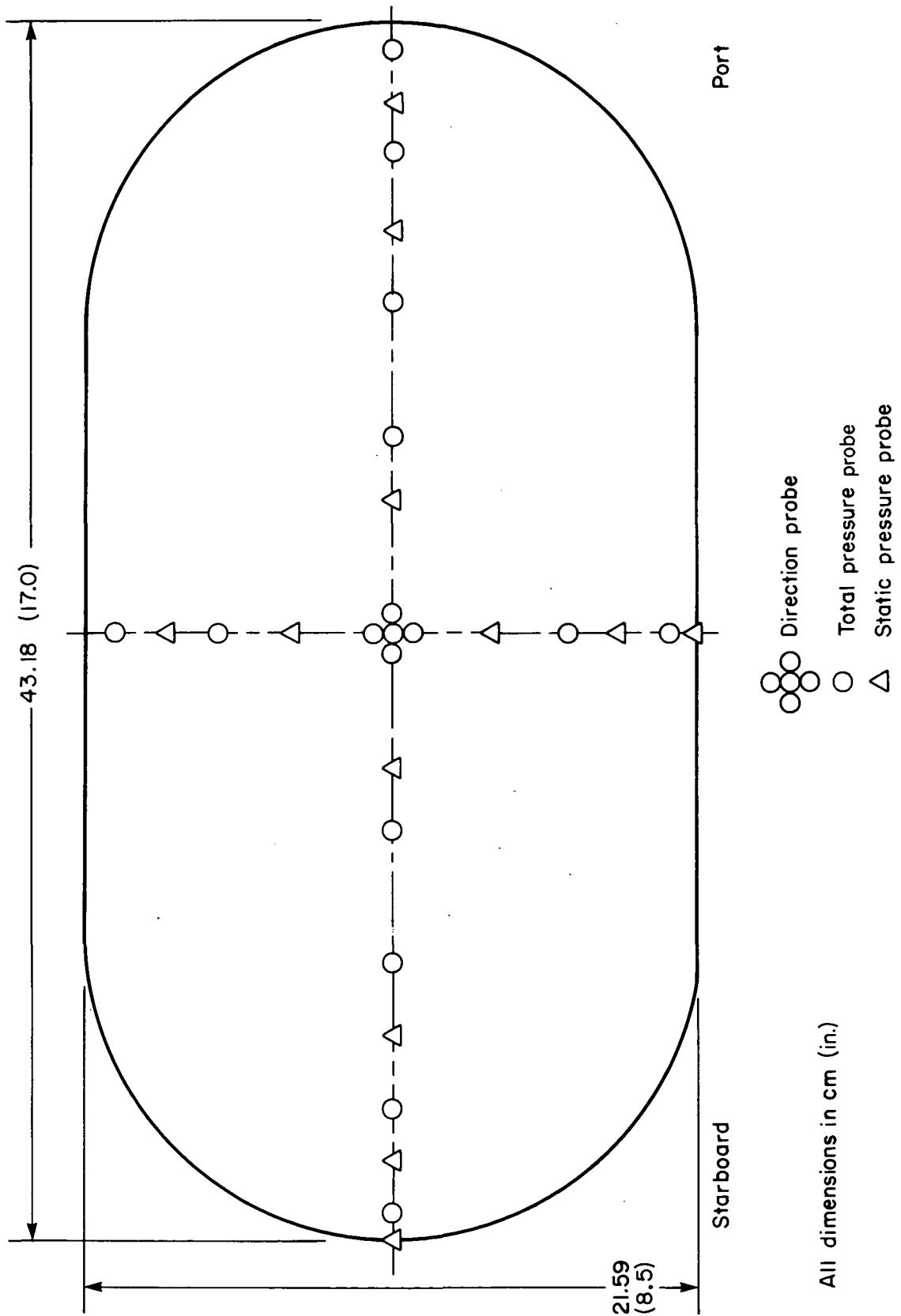


Figure 4.- Test section instrumentation, looking downstream.

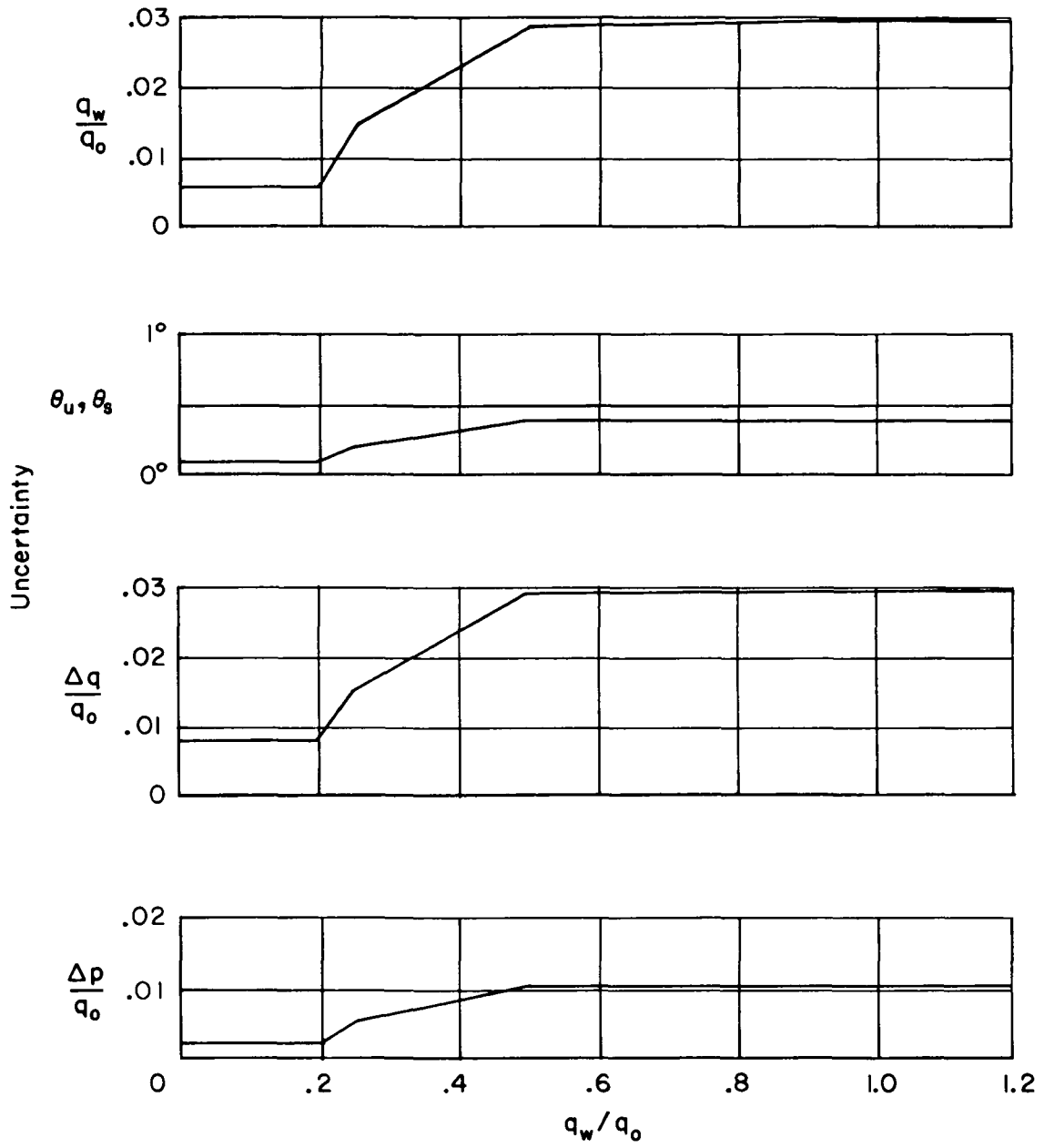
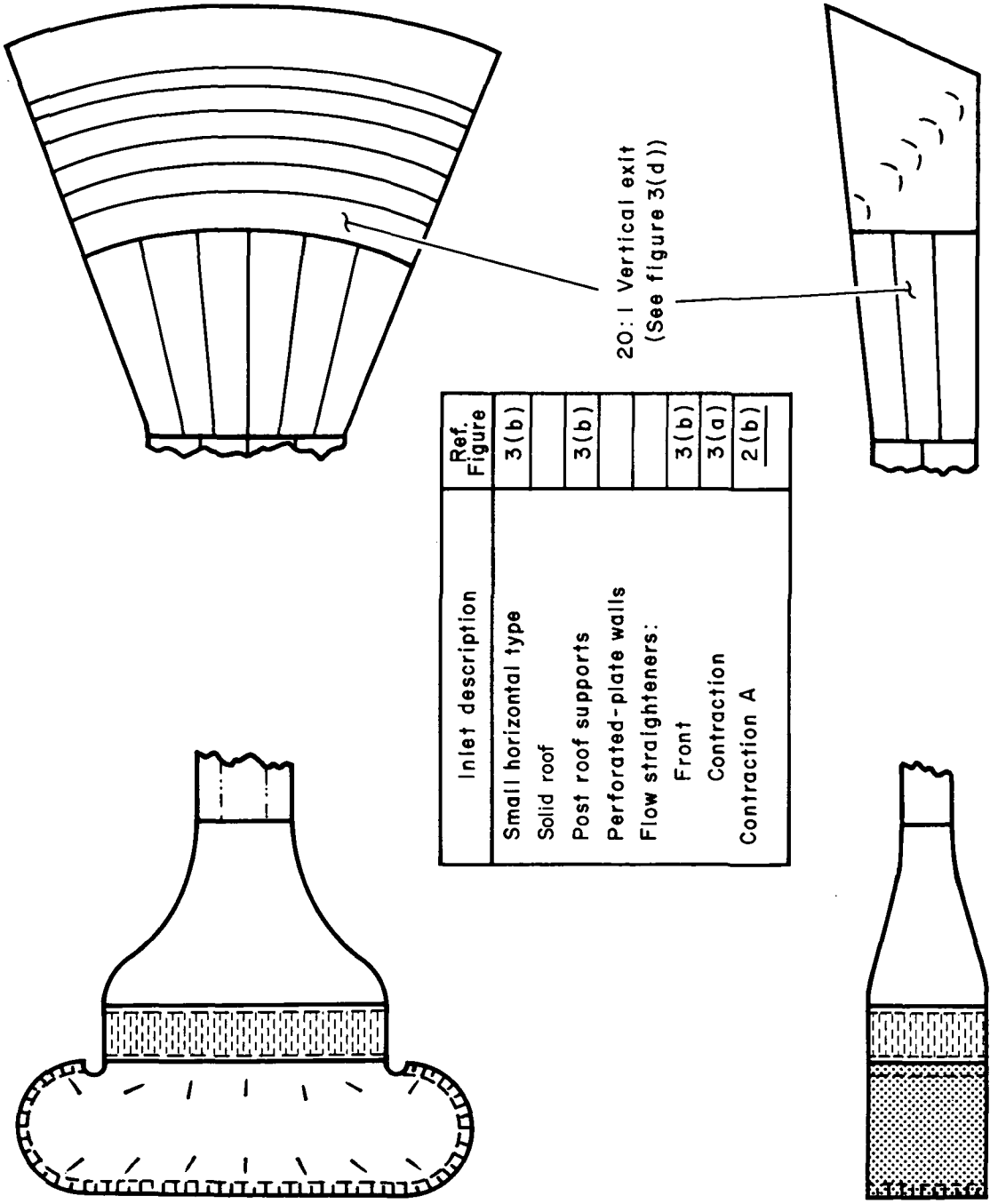
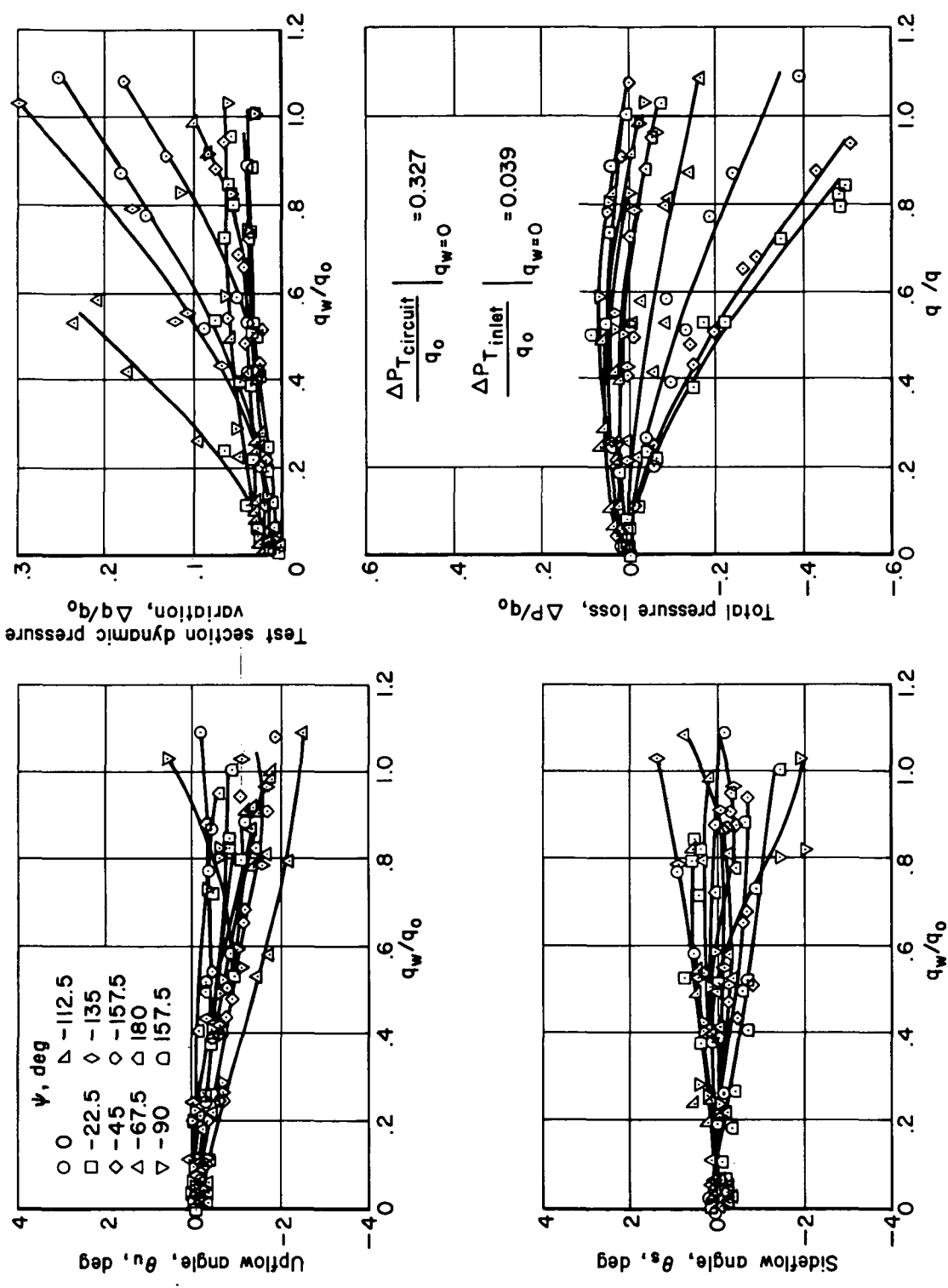


Figure 5.- Experimental uncertainties in the flow quality and performance parameters.



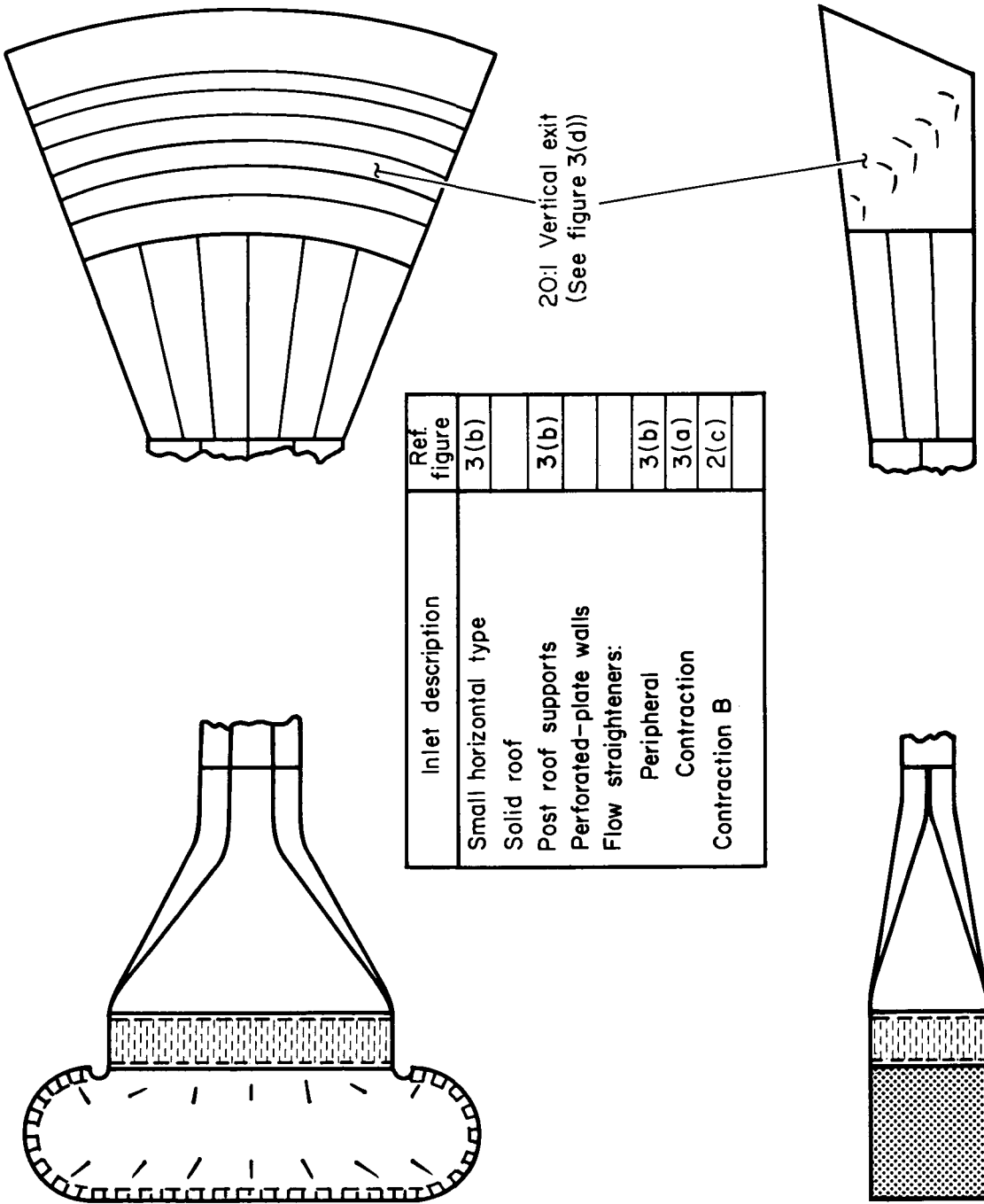
(a) End treatment configurations.

Figure 6.- Circuit with small horizontal inlet with solid roof and post supports, perforated-plate walls, front flow straightener, and with 20:1 vertical exit.



(b) Configuration flow results.

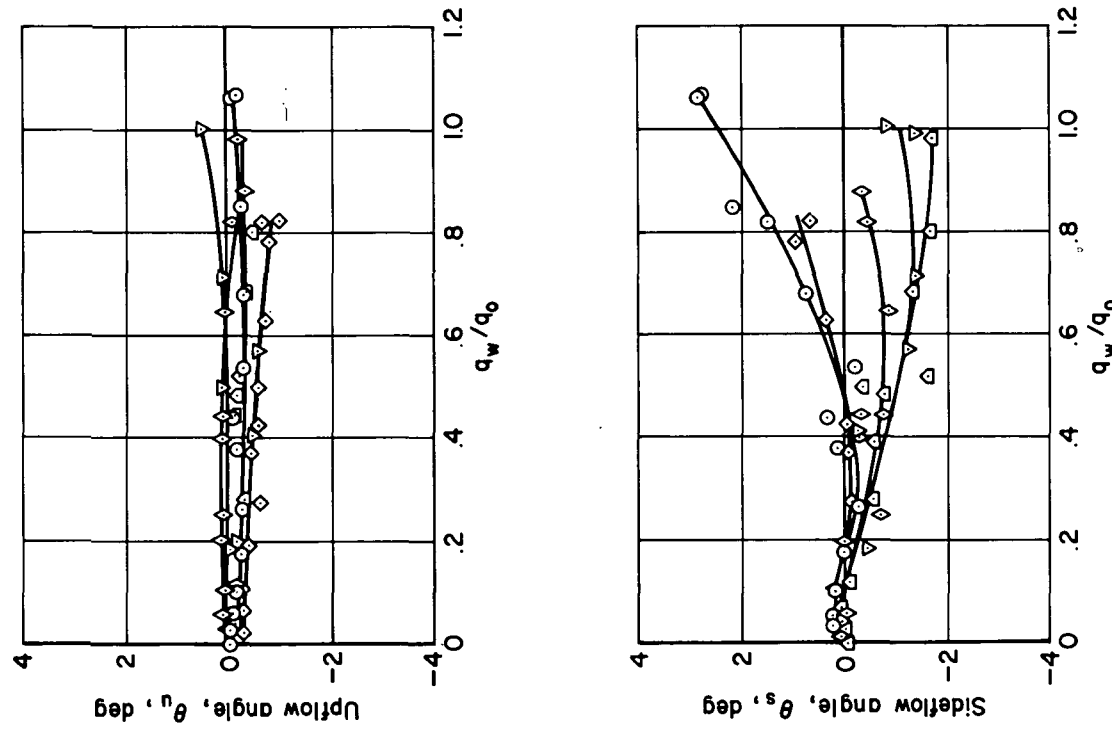
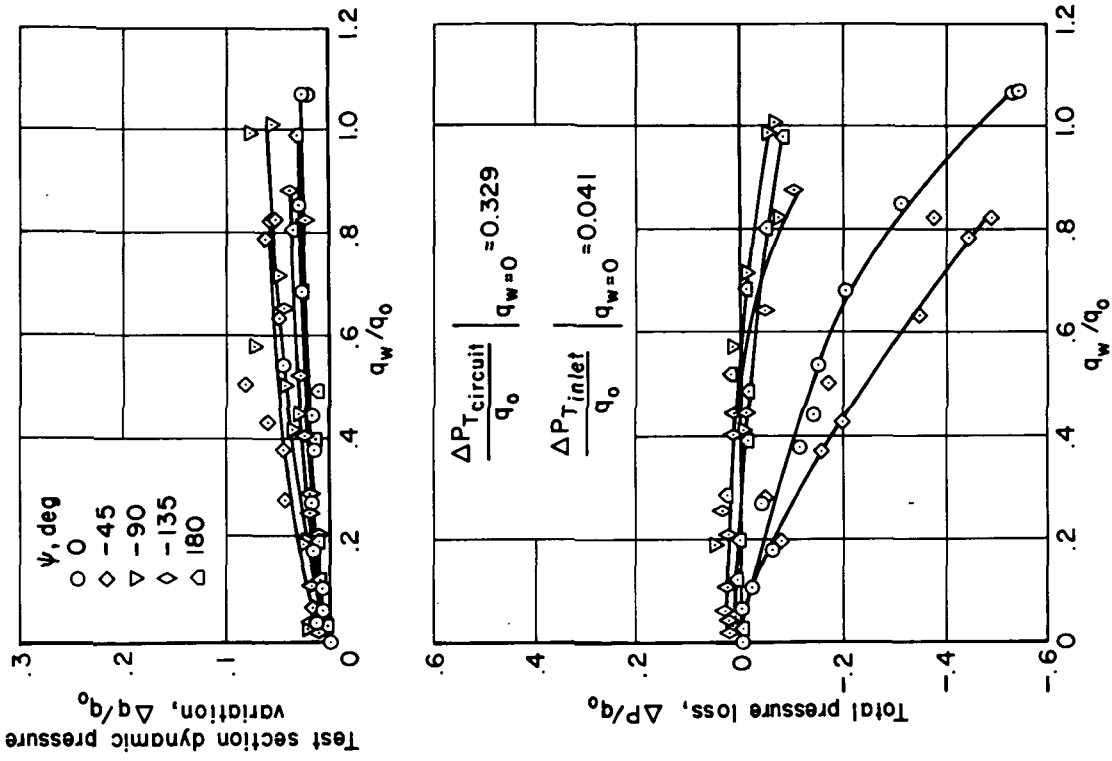
Figure 6.- Concluded.



20:1 Vertical exit
(See figure 3(d))

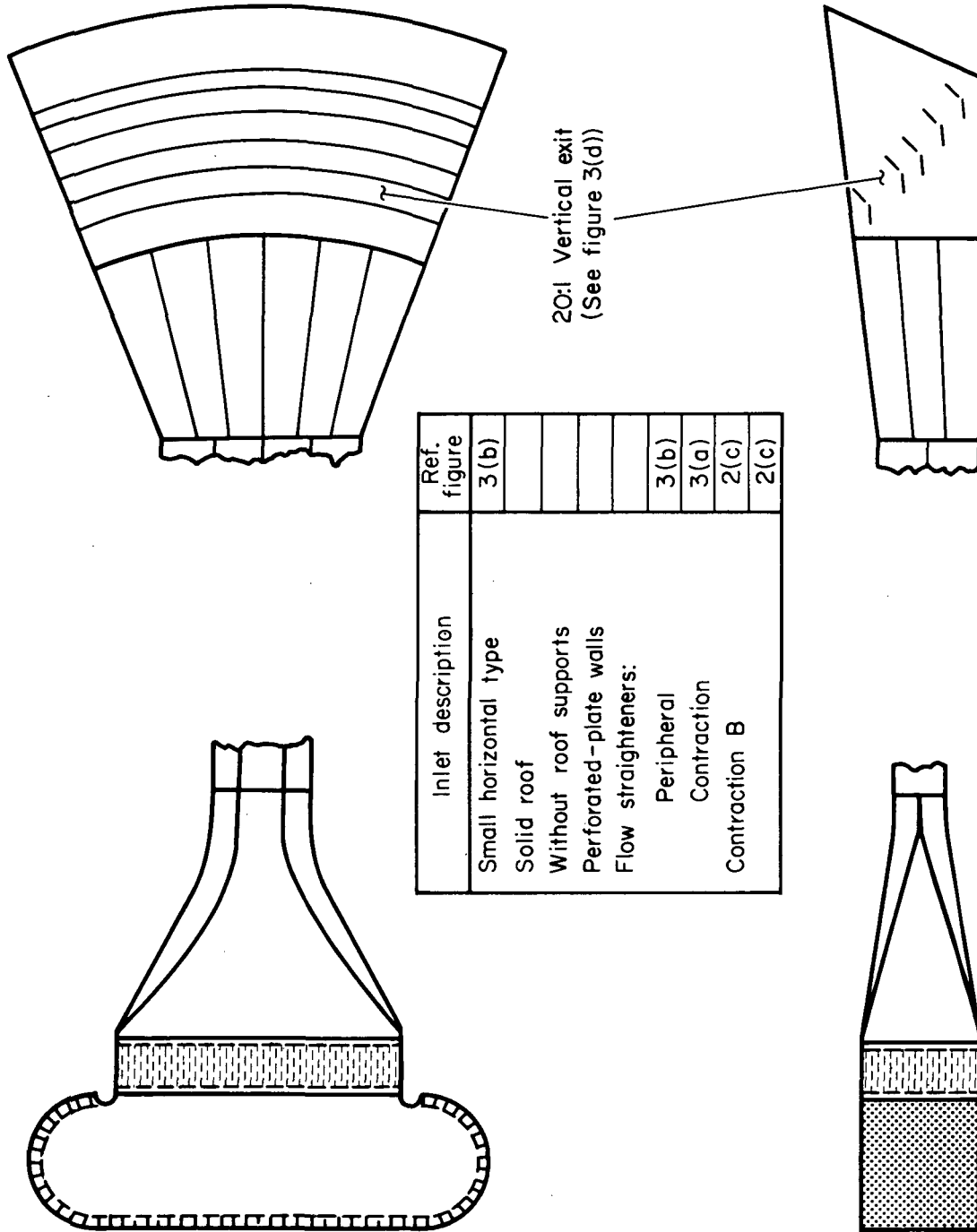
(a) End treatment configurations.

Figure 7.- Circuit with small horizontal inlet with solid roof and post supports, peripheral flow straightener, and with 20:1 vertical exit.



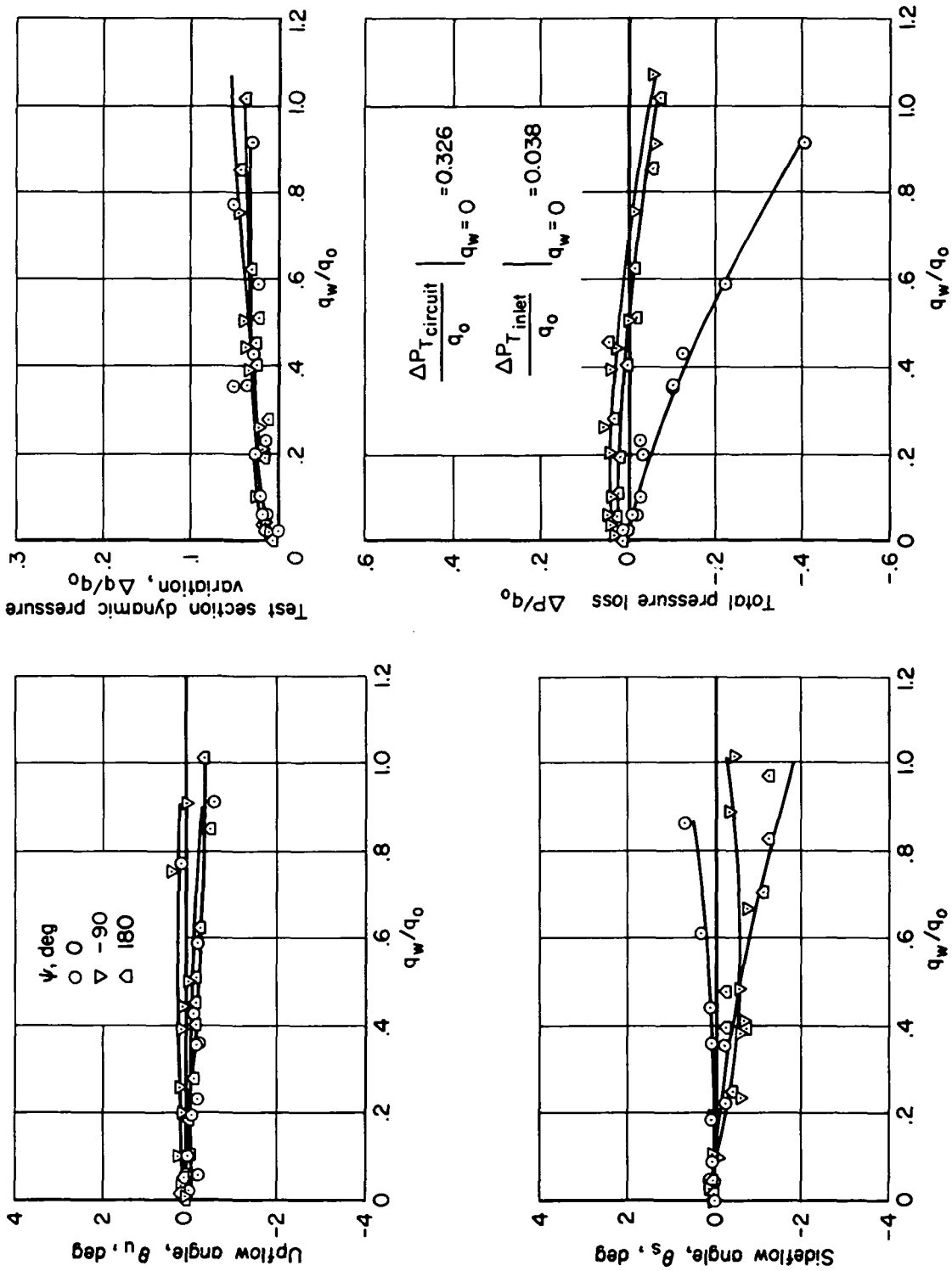
(b) Configuration flow results.

Figure 7.- Concluded.



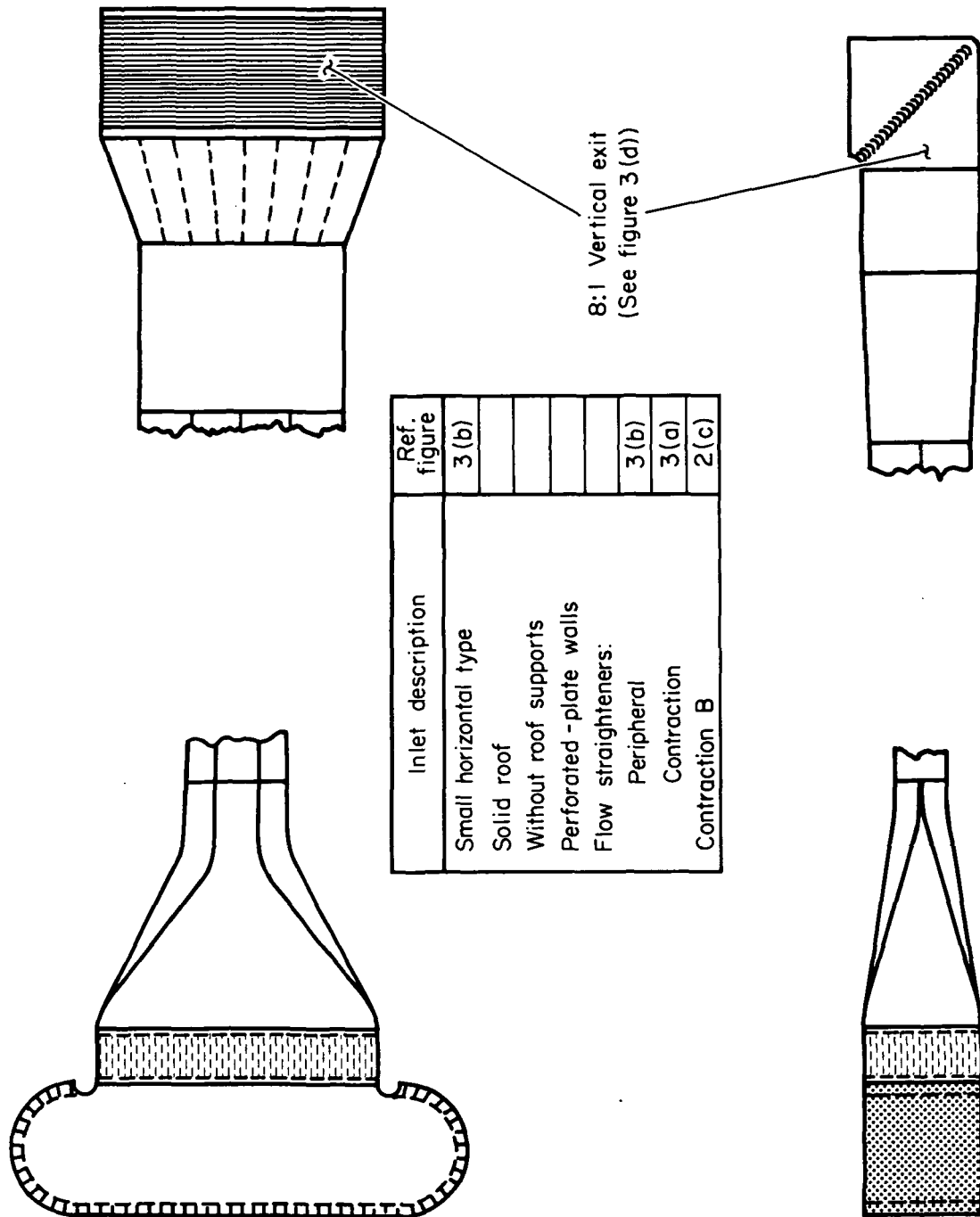
(a) End treatment configurations.

Figure 8.- Circuit with small horizontal inlet with peripheral flow straightener and with 20:1 vertical exit.



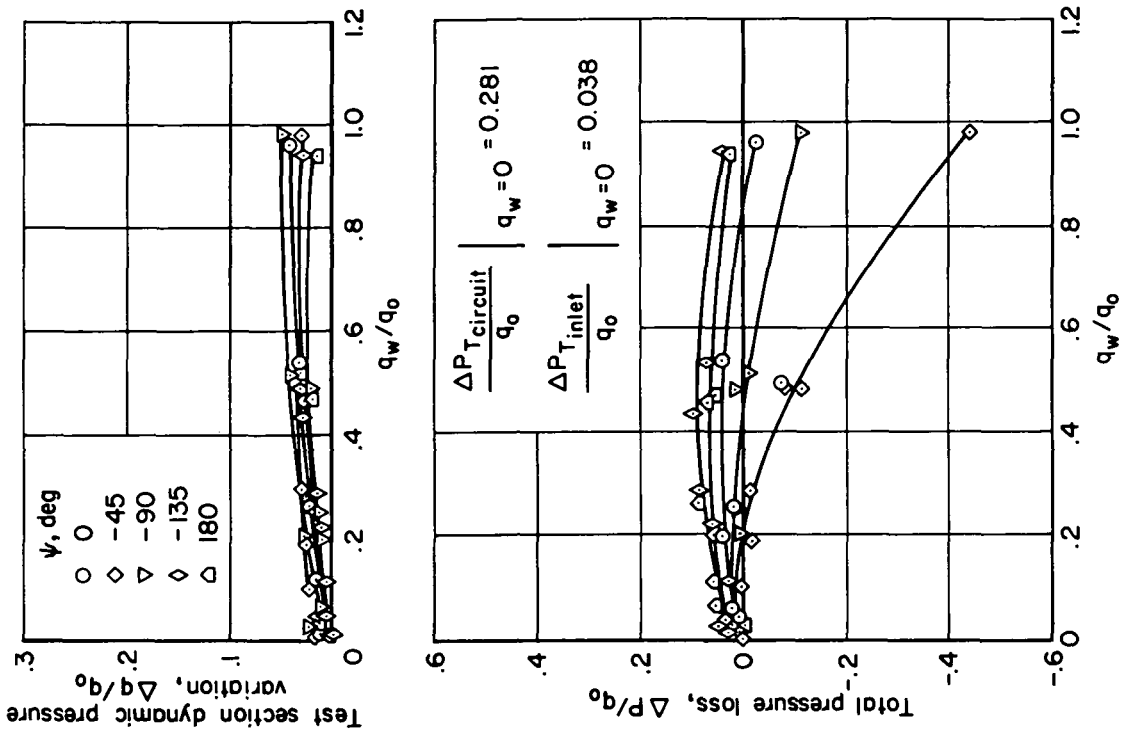
(b) Configuration flow results.

Figure 8. - Concluded.



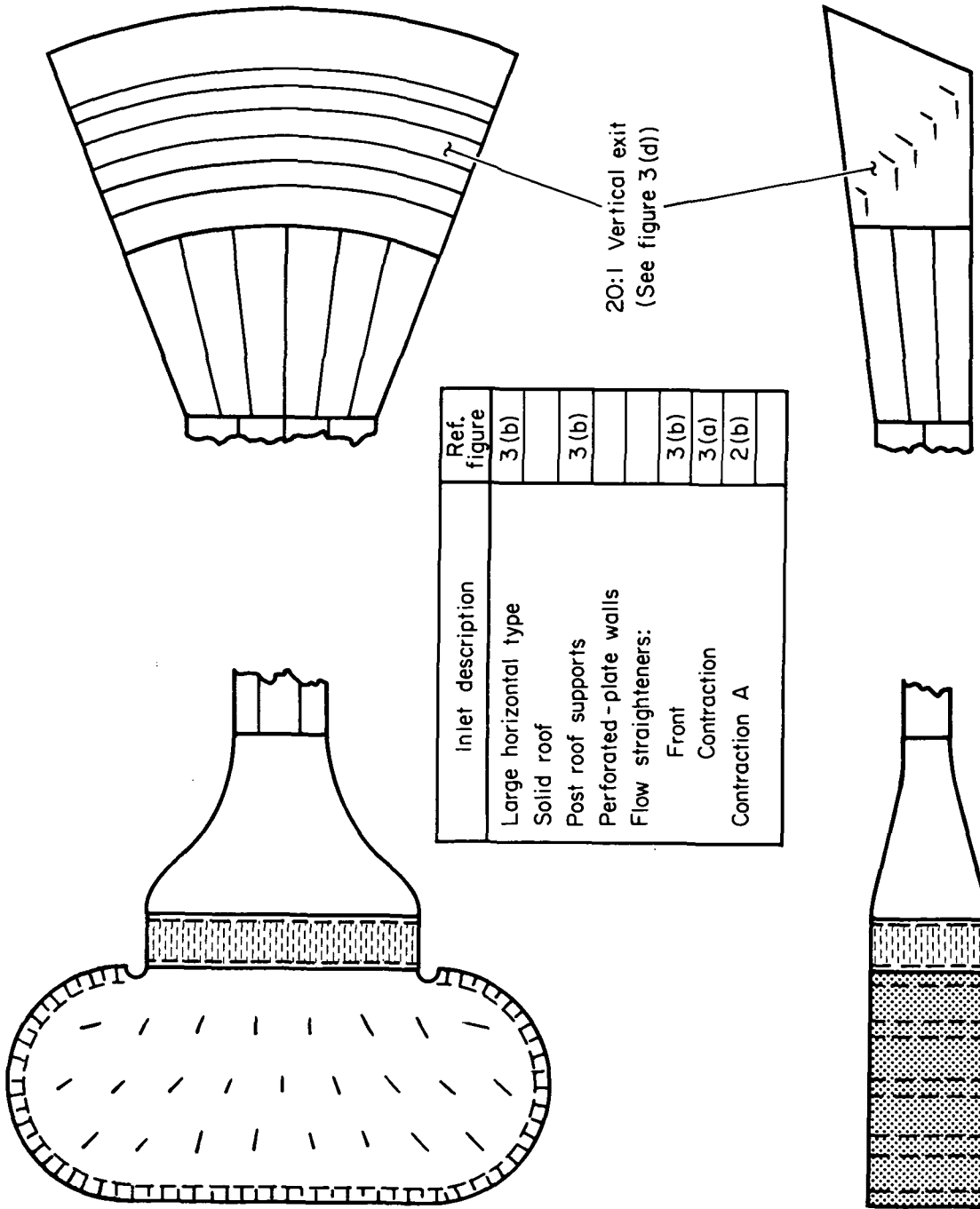
(a) End treatment configurations.

Figure 9.- Circuit with small horizontal inlet with peripheral flow straightener and with 8:1 vertical exit.



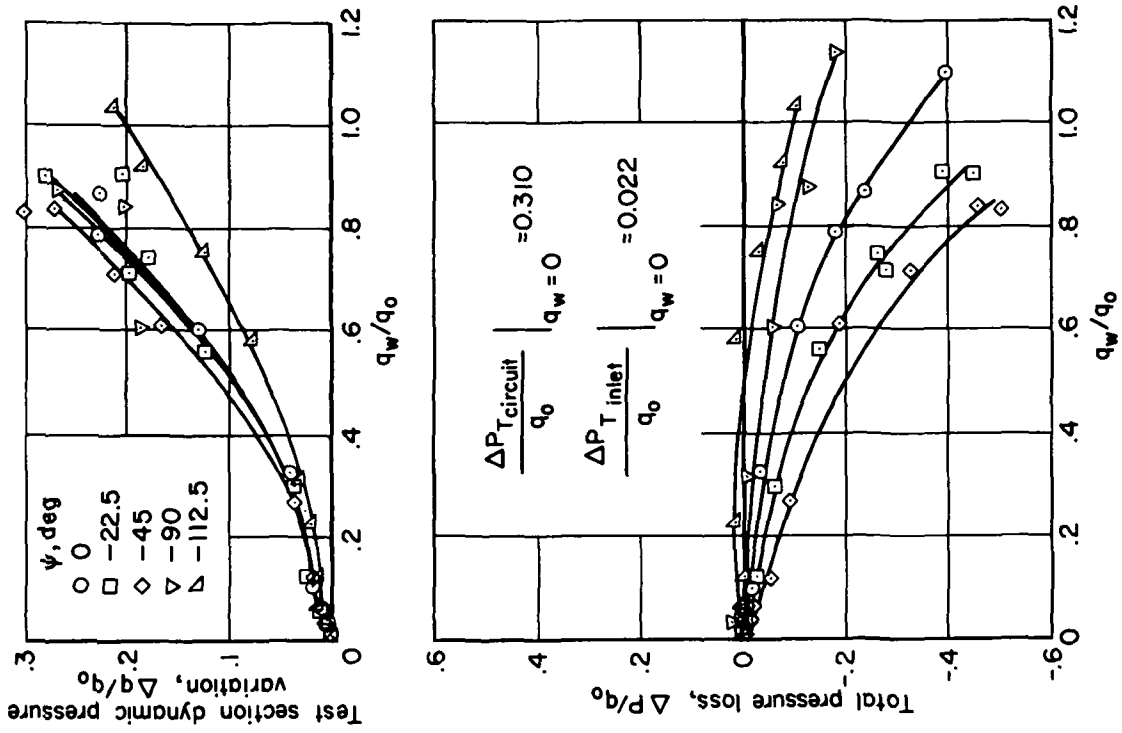
(b) Configuration flow results.

Figure 9.- Concluded.



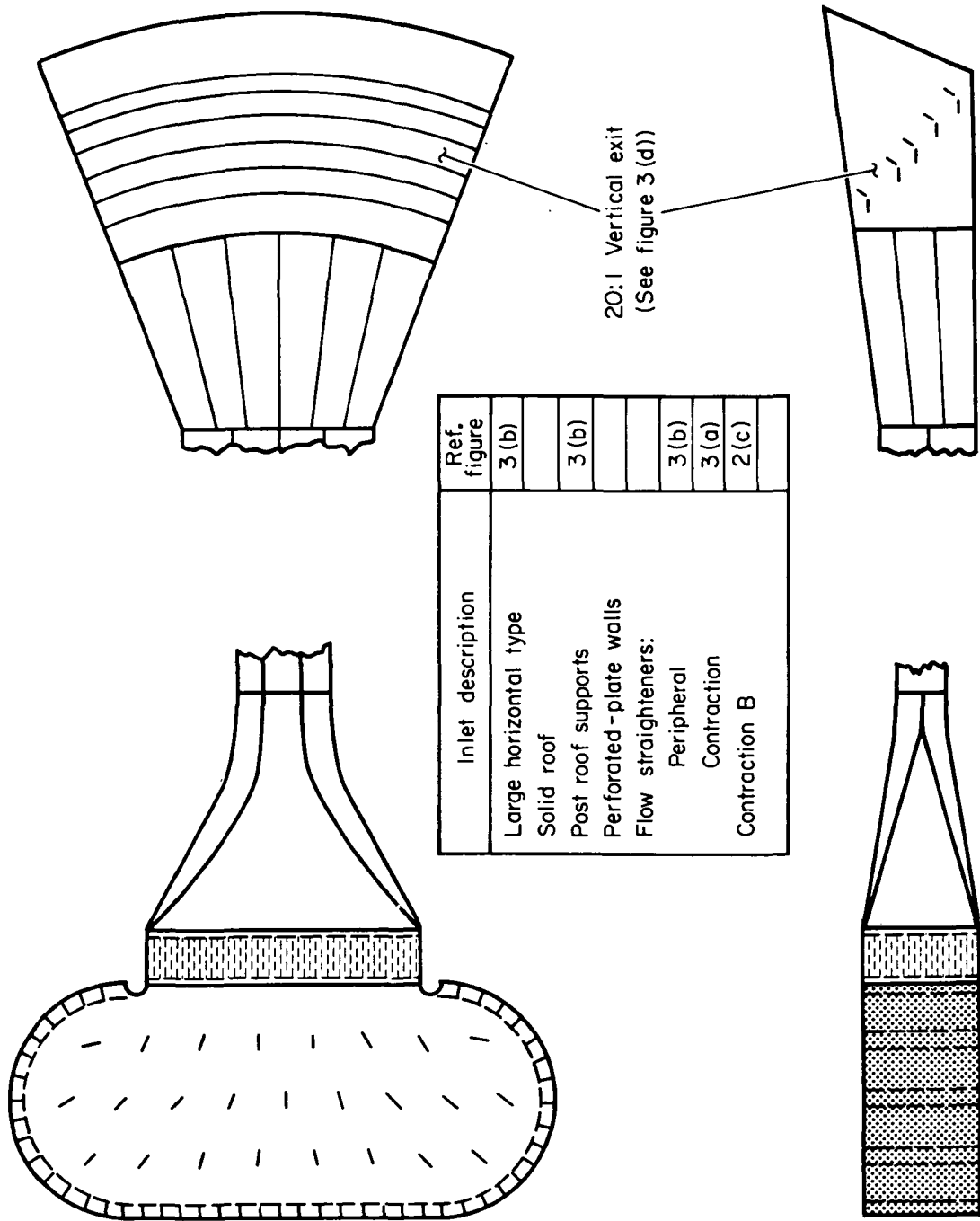
(a) End treatment configurations.

Figure 10.- Circuit with large horizontal inlet with solid roof and post supports, front flow straightener, and with 20:1 vertical exit.



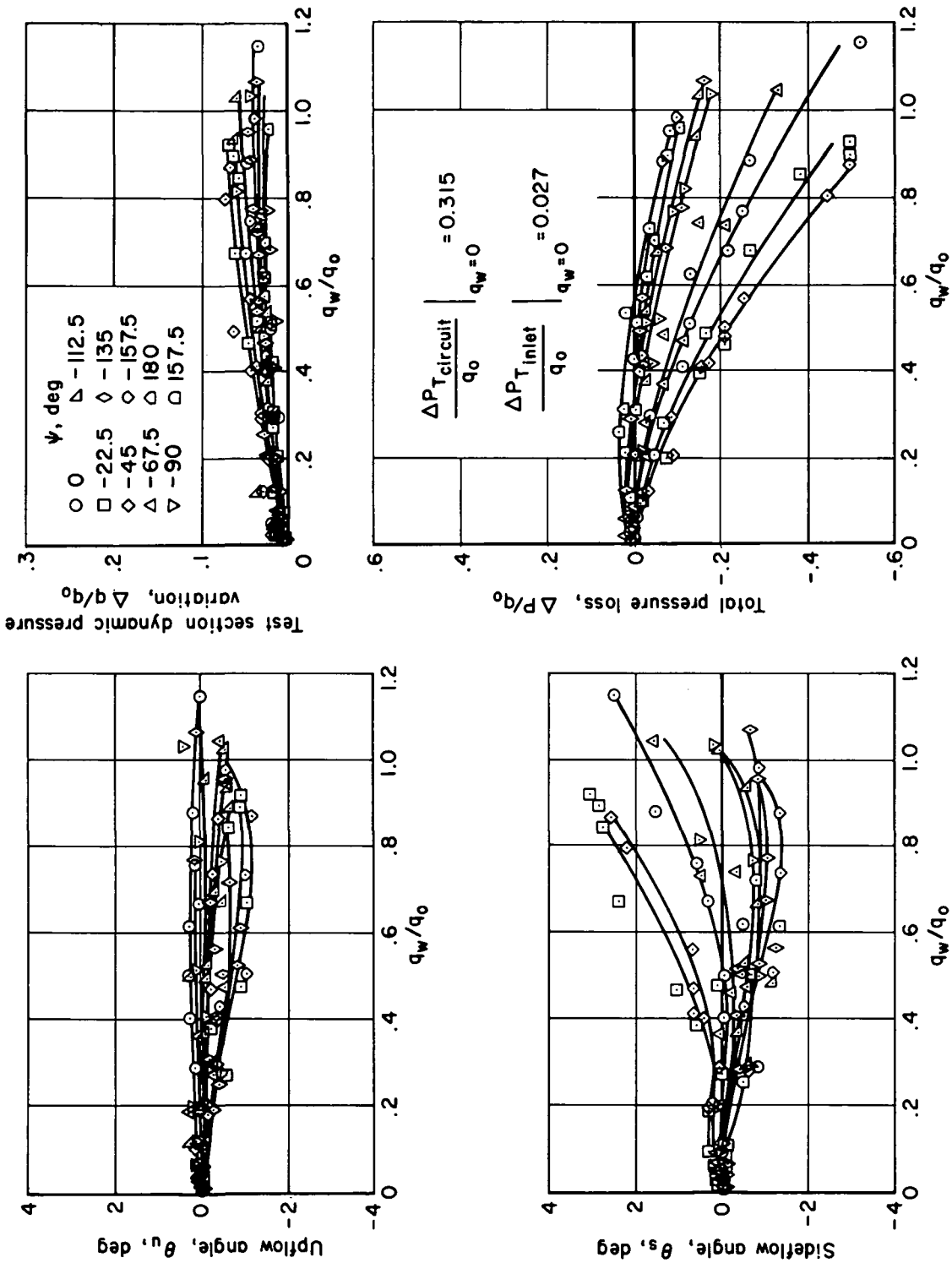
(b) Configuration flow results.

Figure 10.- Concluded.



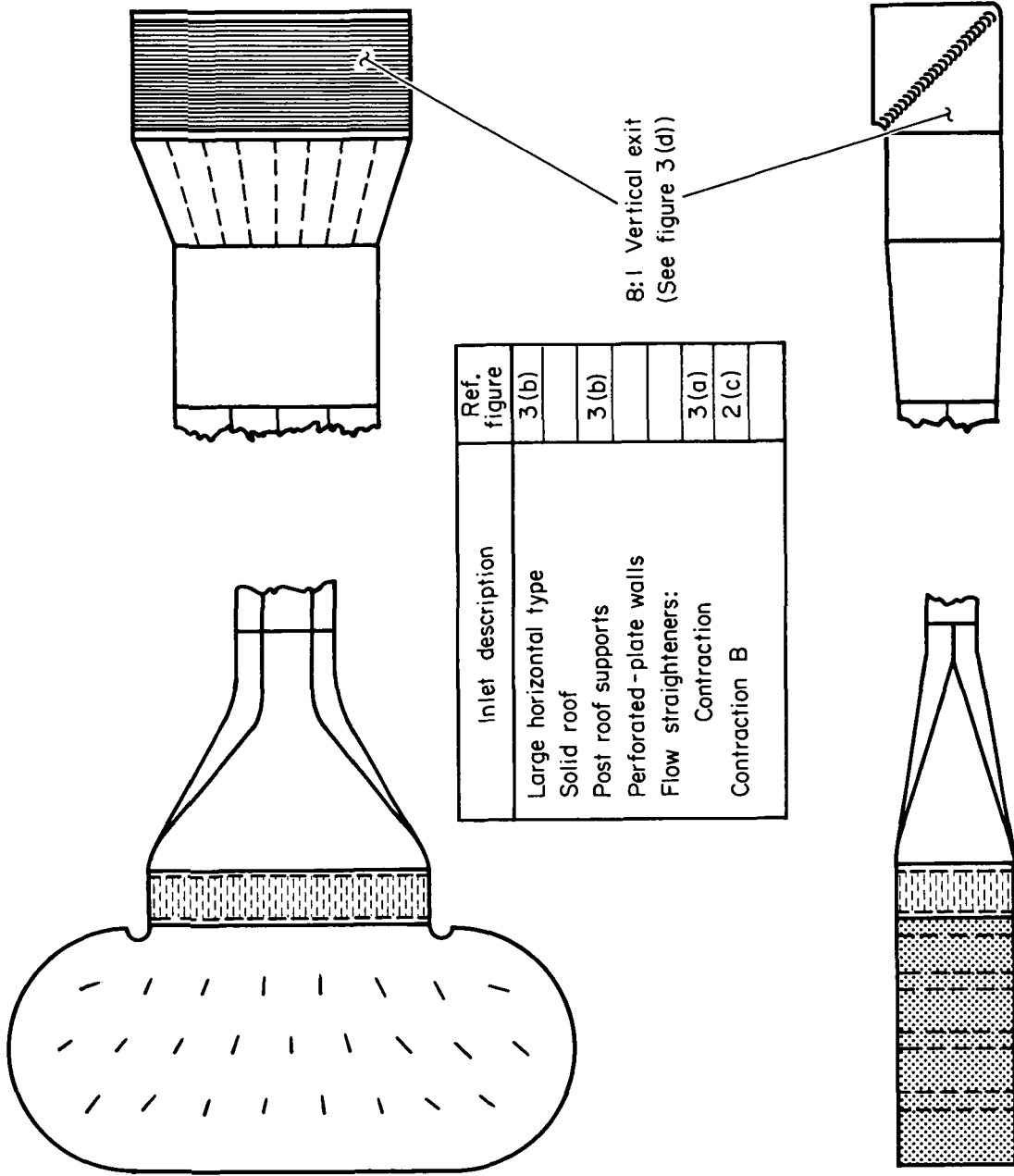
(a) End treatment configurations.

Figure 11.- Circuit with large horizontal inlet with solid roof and post supports, peripheral flow straightener, and with 20:1 vertical exit.



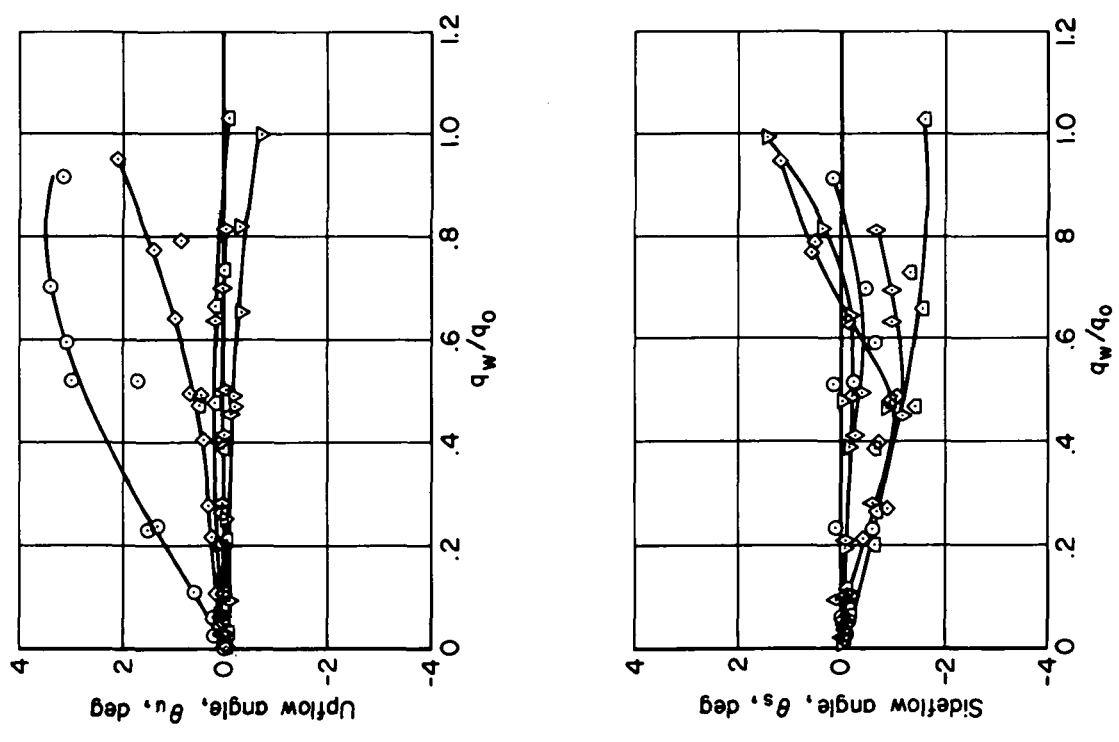
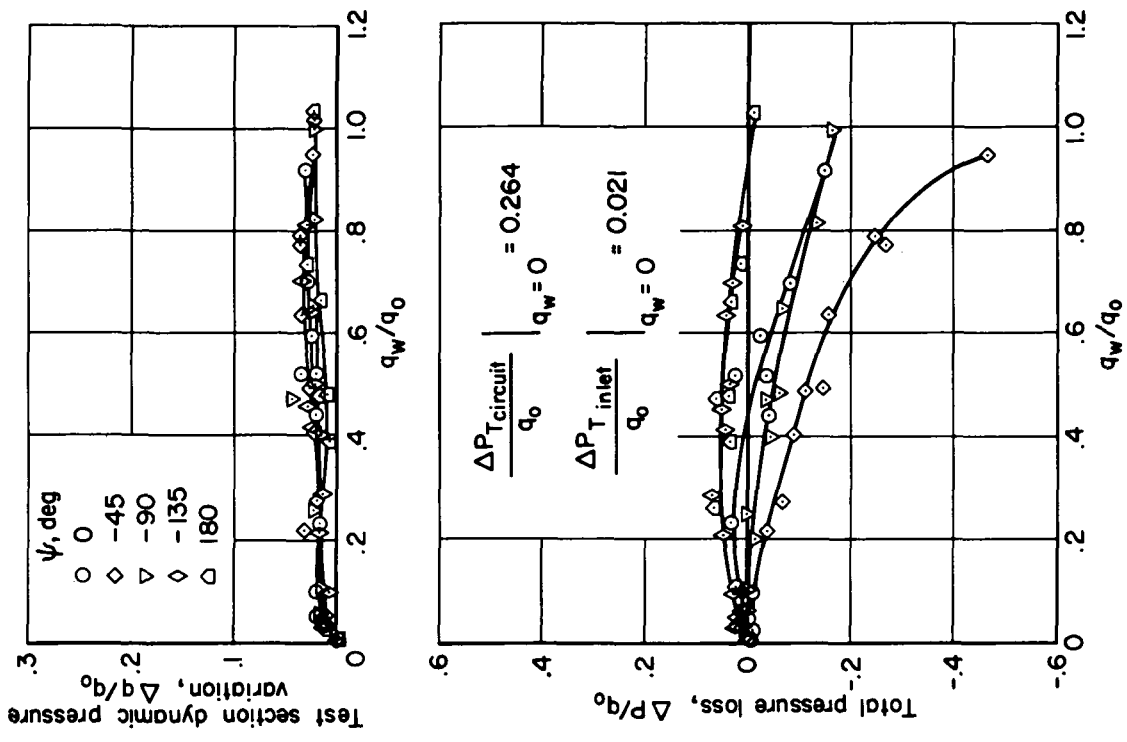
(b) Configuration flow results.

Figure 11.- Concluded.



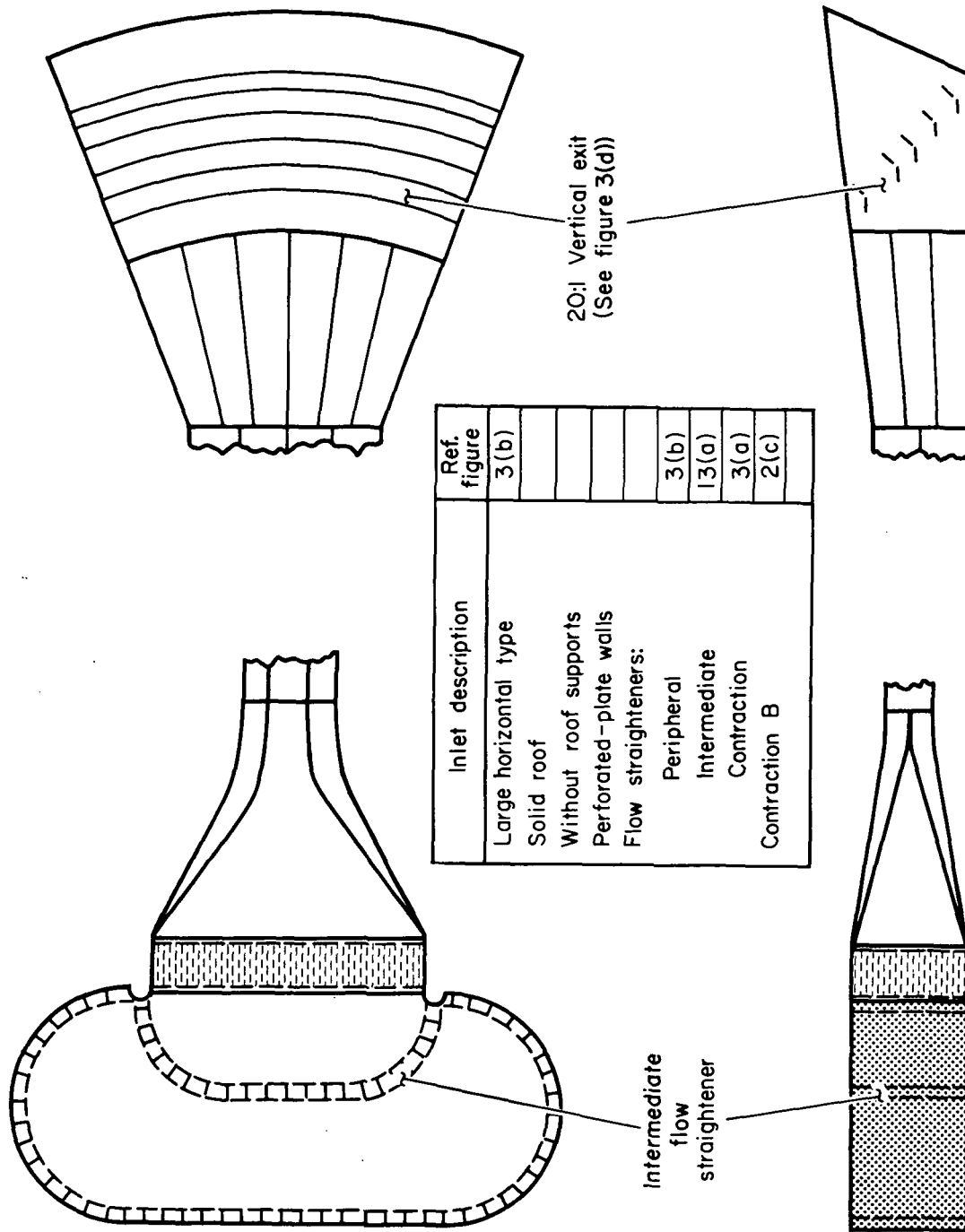
(a) End treatment configurations.

Figure 12.- Circuit with large horizontal inlet with solid roof and post supports, and with 8:1 vertical exit.



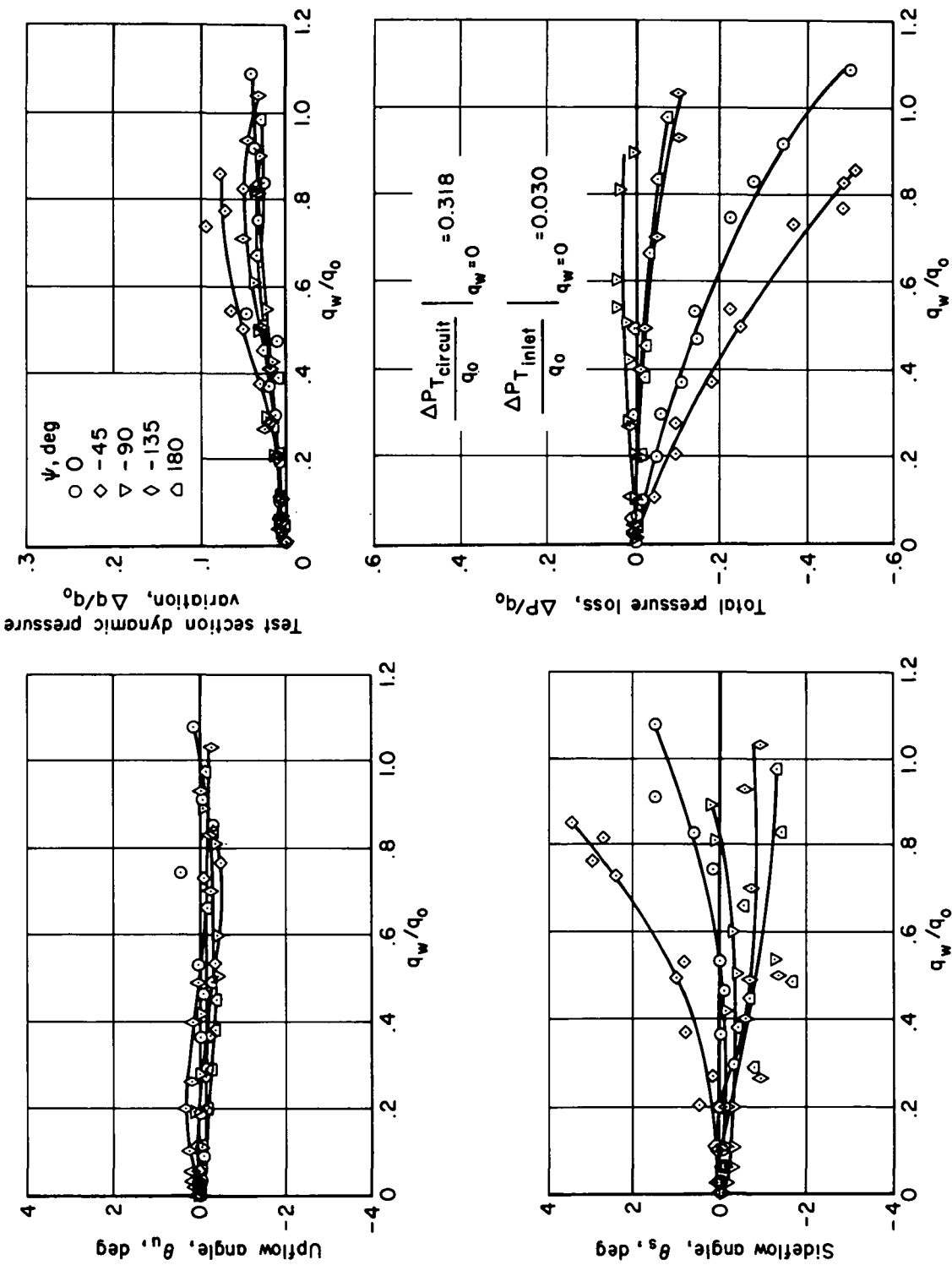
(b) Configuration flow results.

Figure 12.- Concluded.



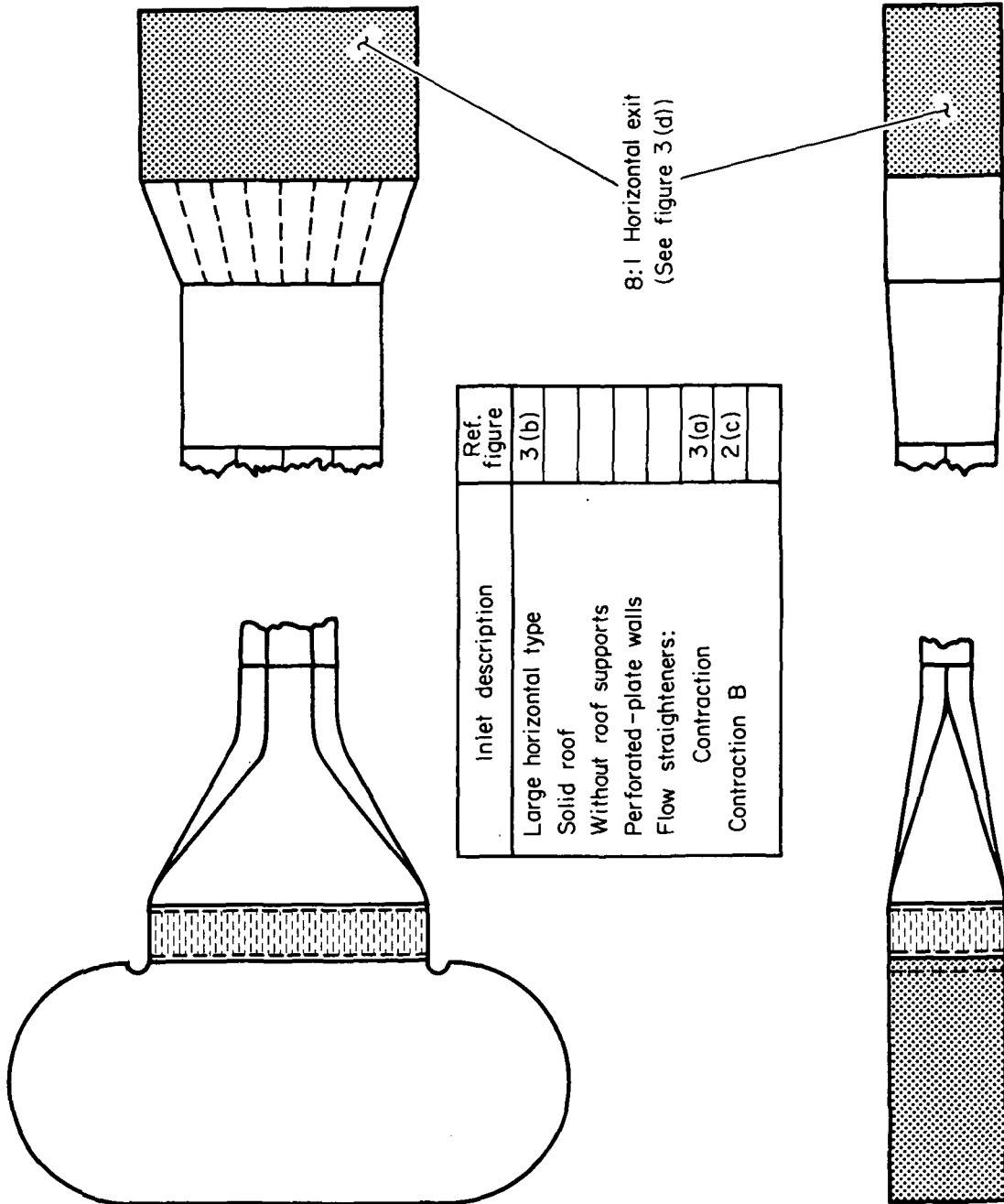
(a) End treatment configurations.

Figure 13.- Circuit with large horizontal inlet with peripheral and intermediate flow straighteners, and with 20:1 vertical exit.



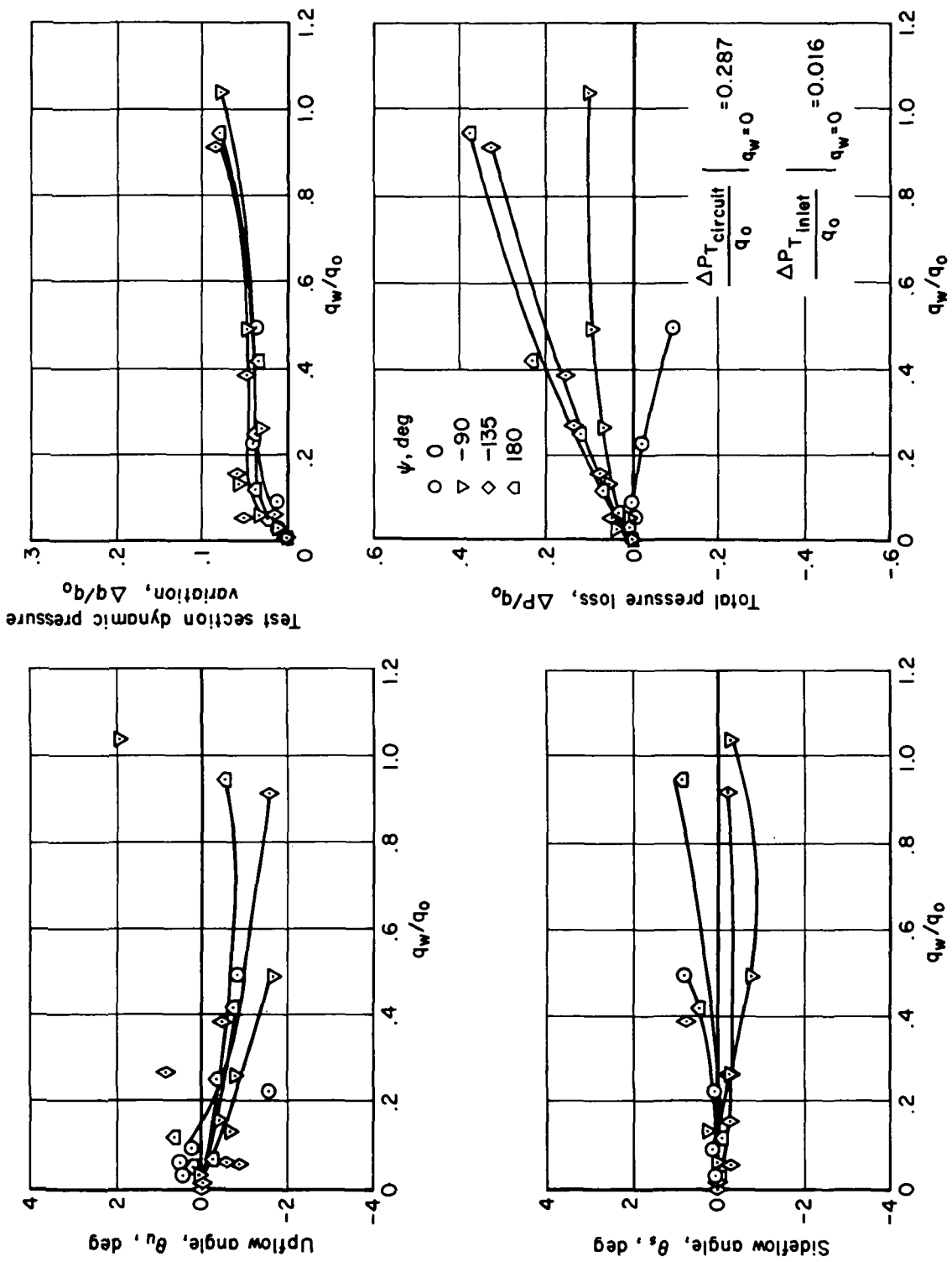
(b) Configuration flow results.

Figure 13.- Concluded.



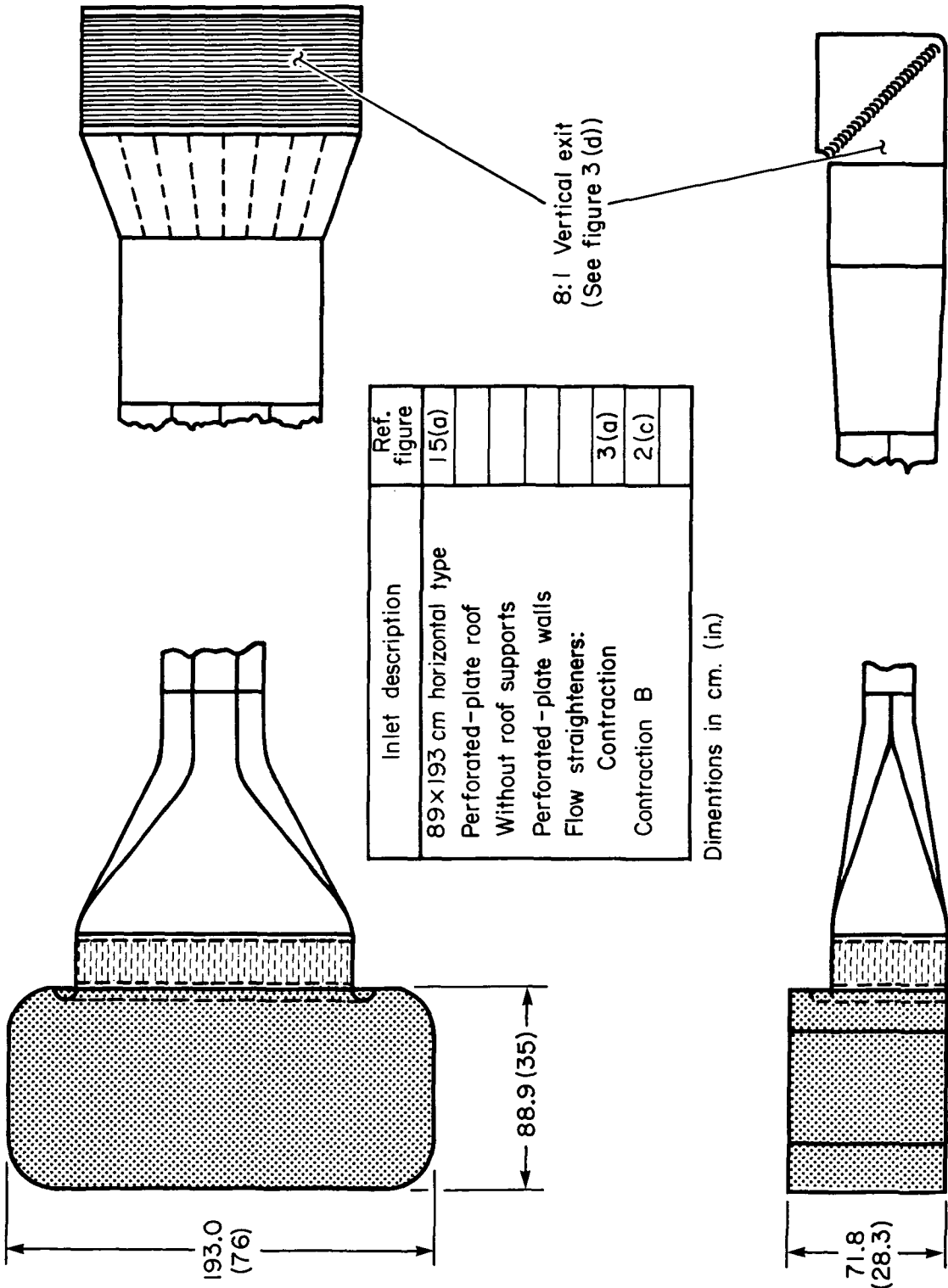
(a) End treatment configurations.

Figure 14. - Circuit with large horizontal inlet and with 8:1 horizontal exit.



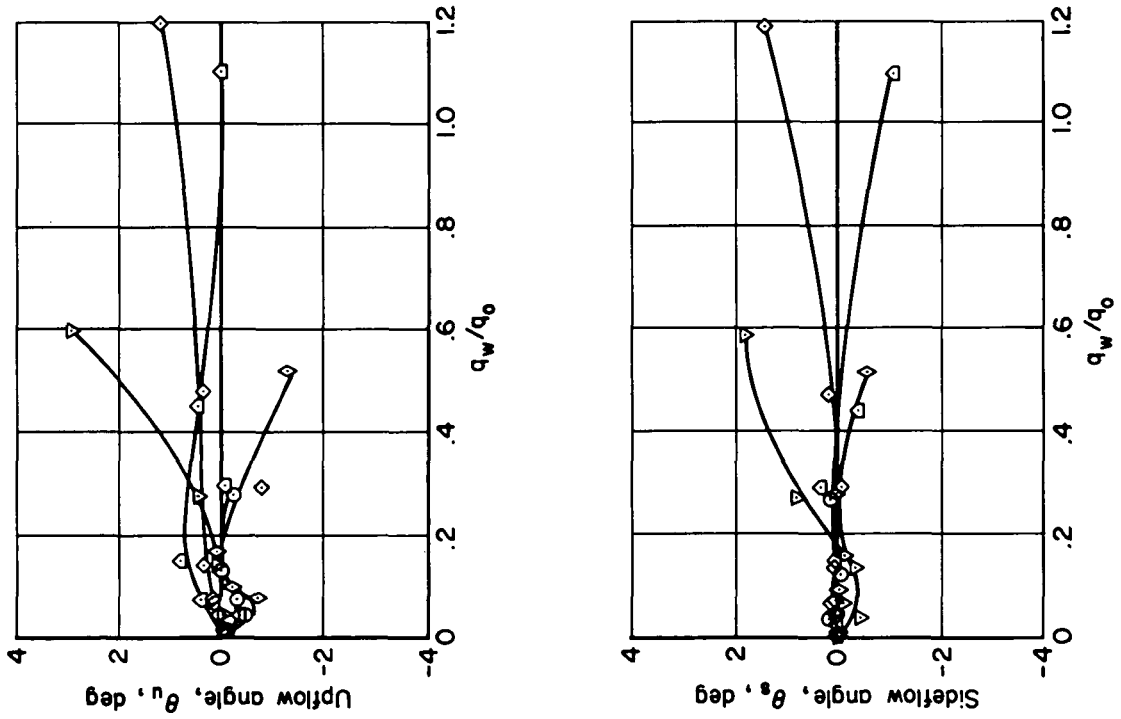
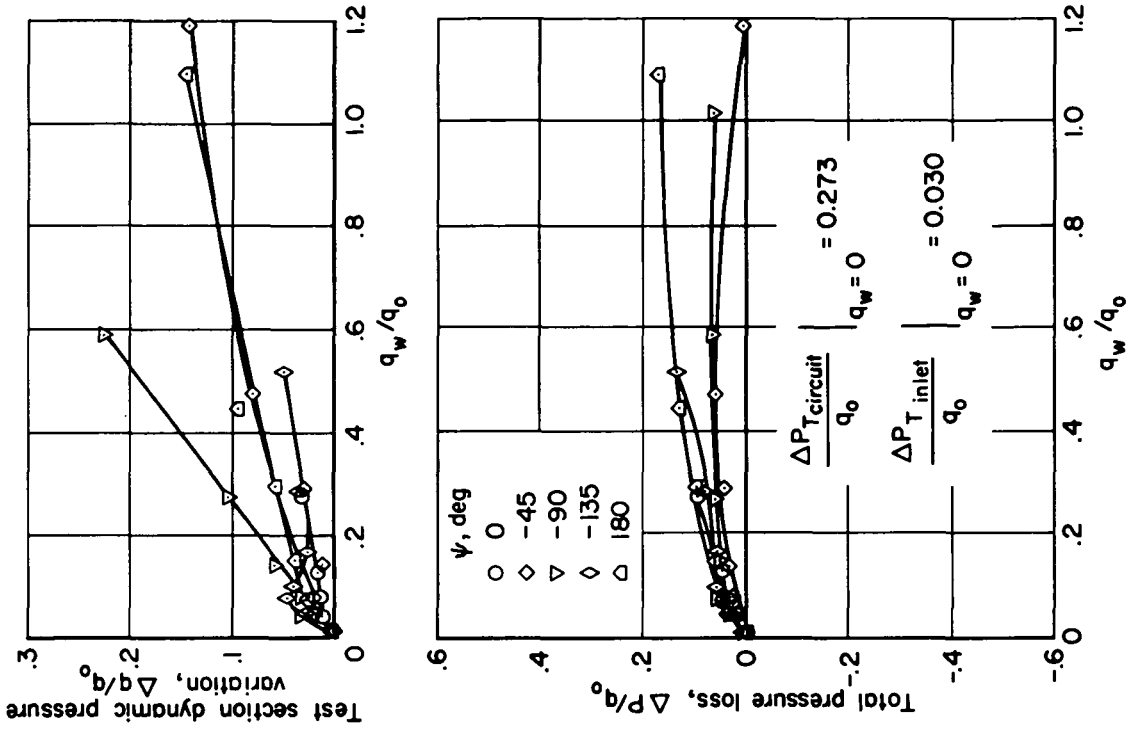
(b) Configuration flow results.

Figure 14.- Concluded.



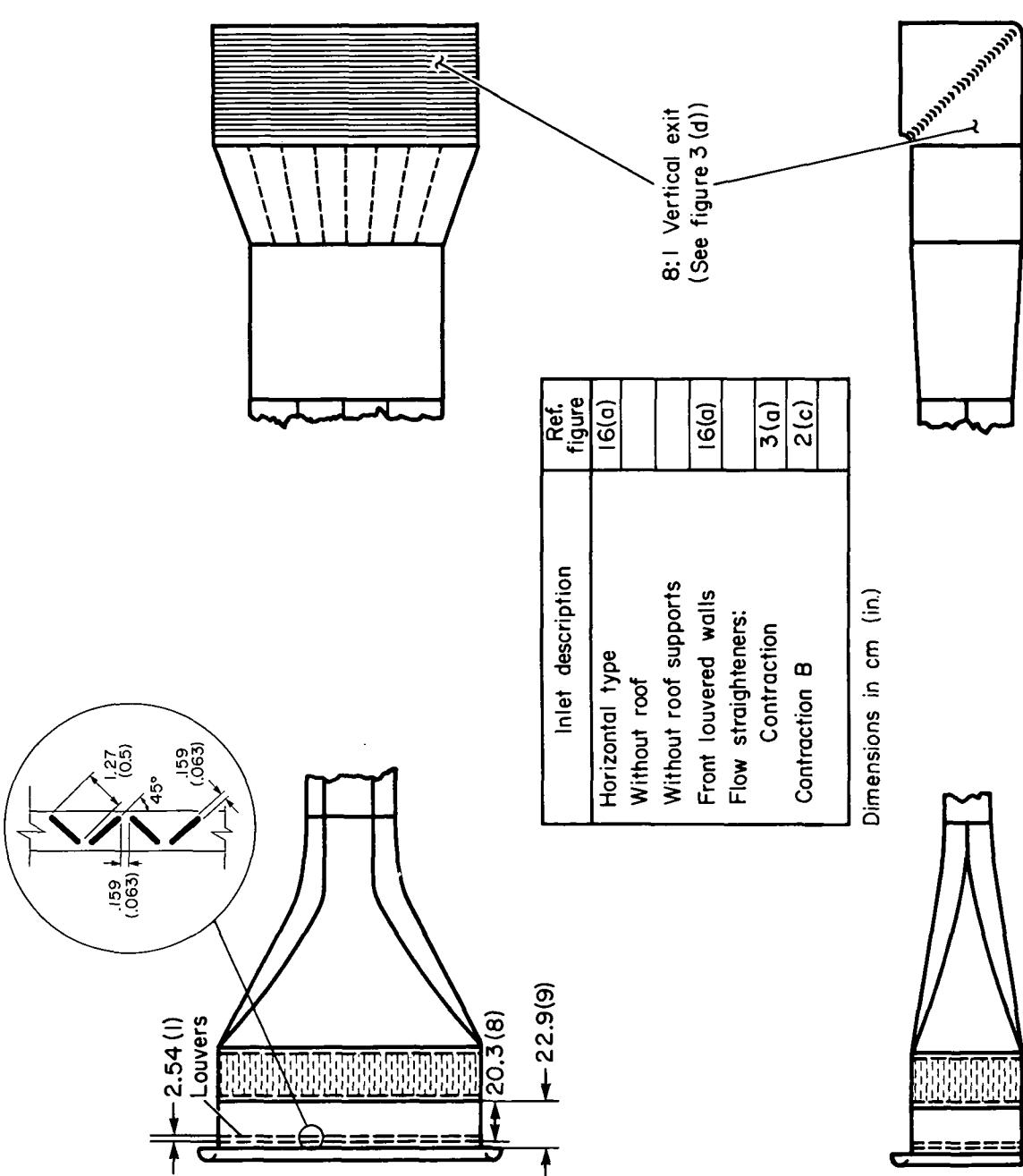
(a) End treatment configuration.

Figure 15.- Circuit with rectangular horizontal inlet with 8:1 vertical exit.



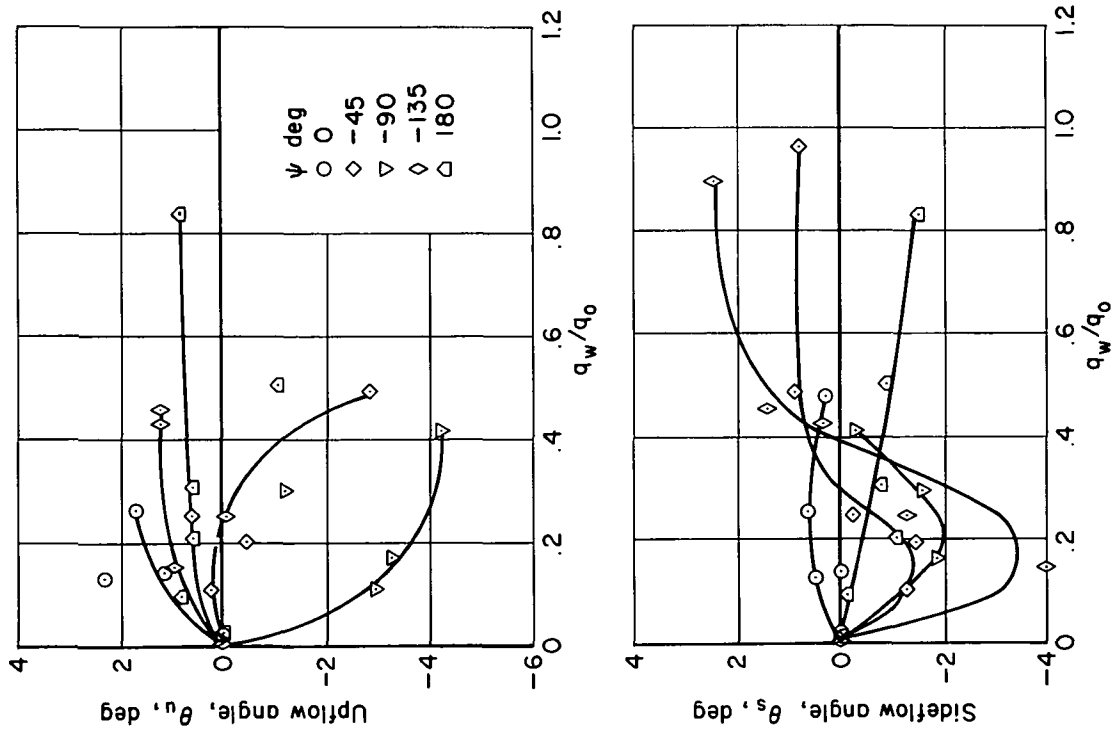
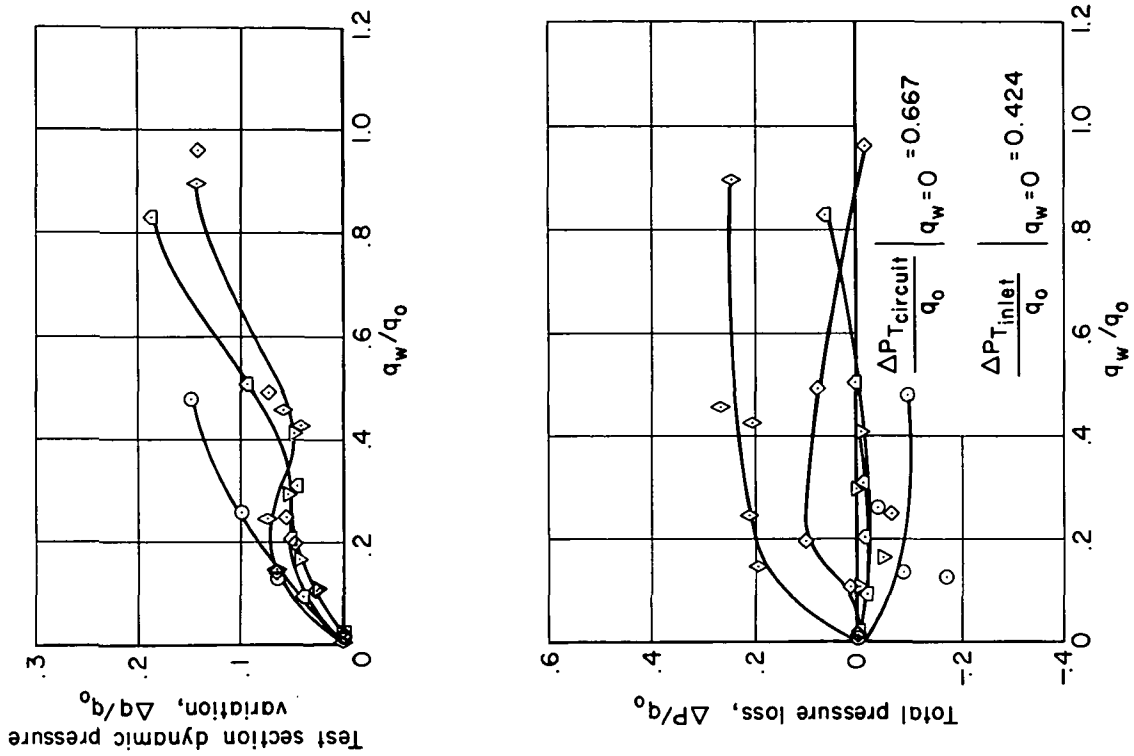
(b) Configuration flow results.

Figure 15.- Concluded.



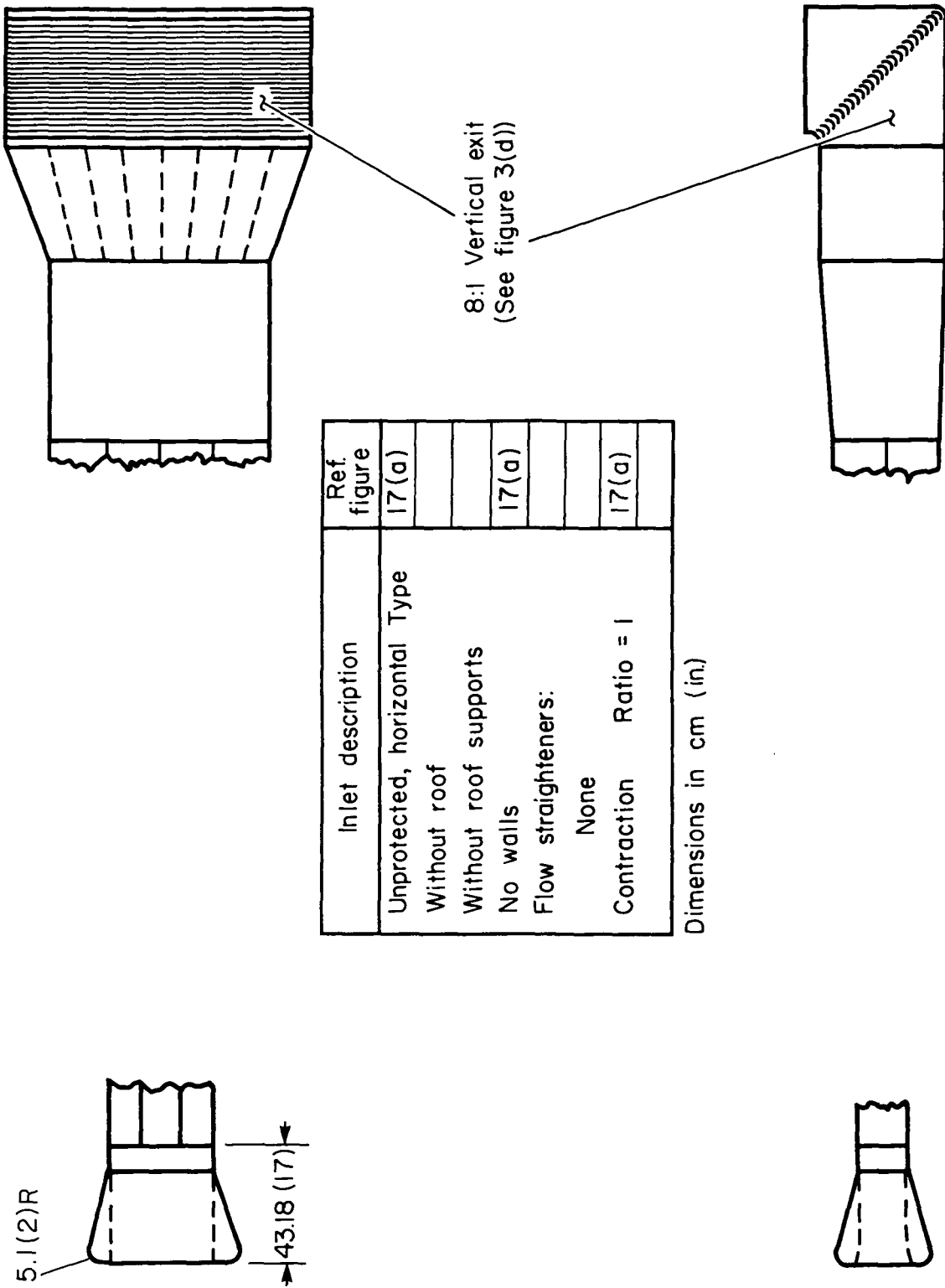
(a) End treatment configuration.

Figure 16.- Circuit with horizontal inlet with front louvers and 8:1 vertical exit.



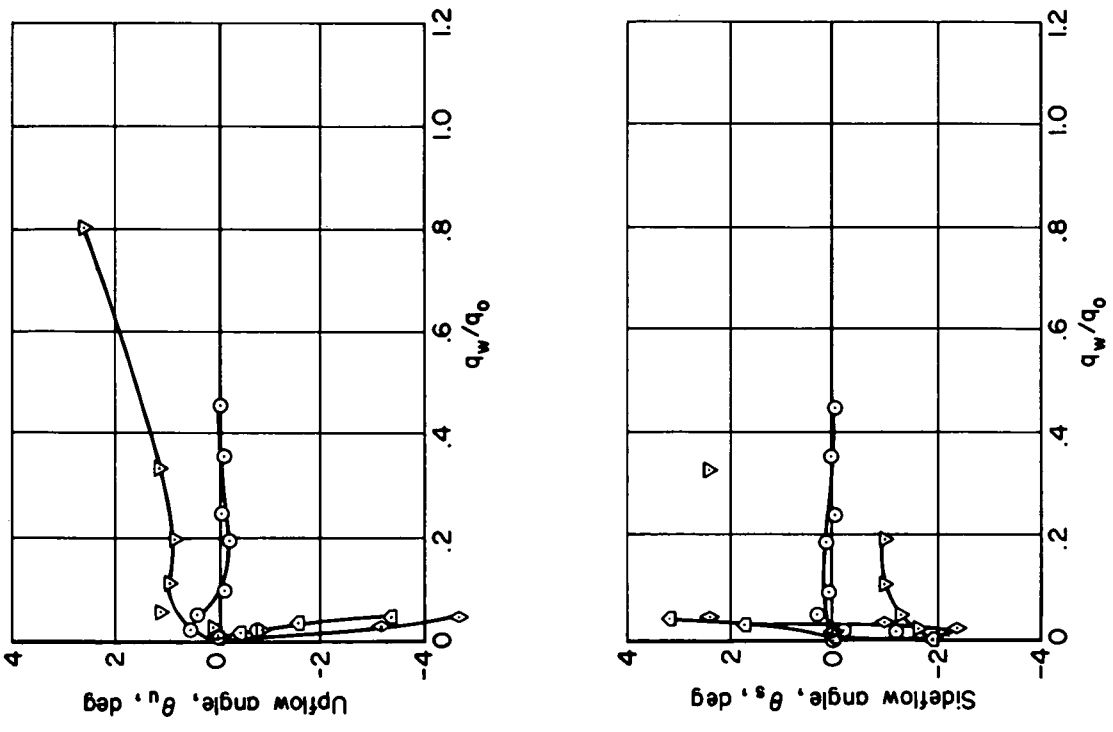
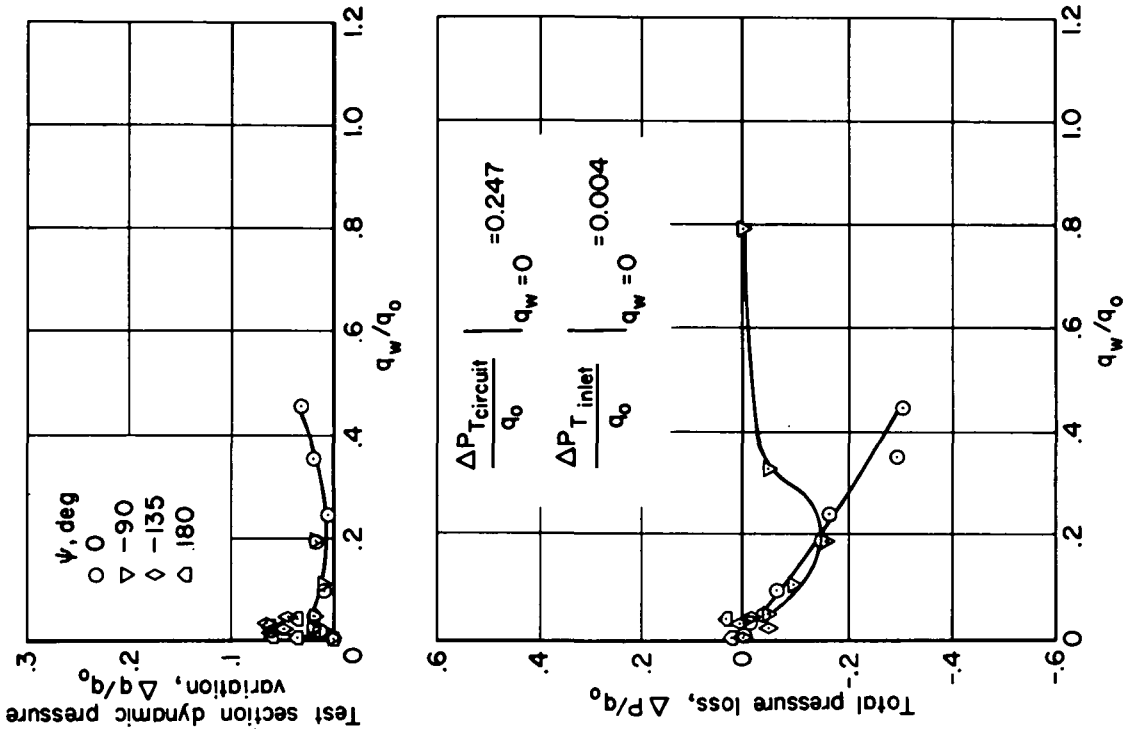
(b) Configuration flow results.

Figure 16.- Concluded.



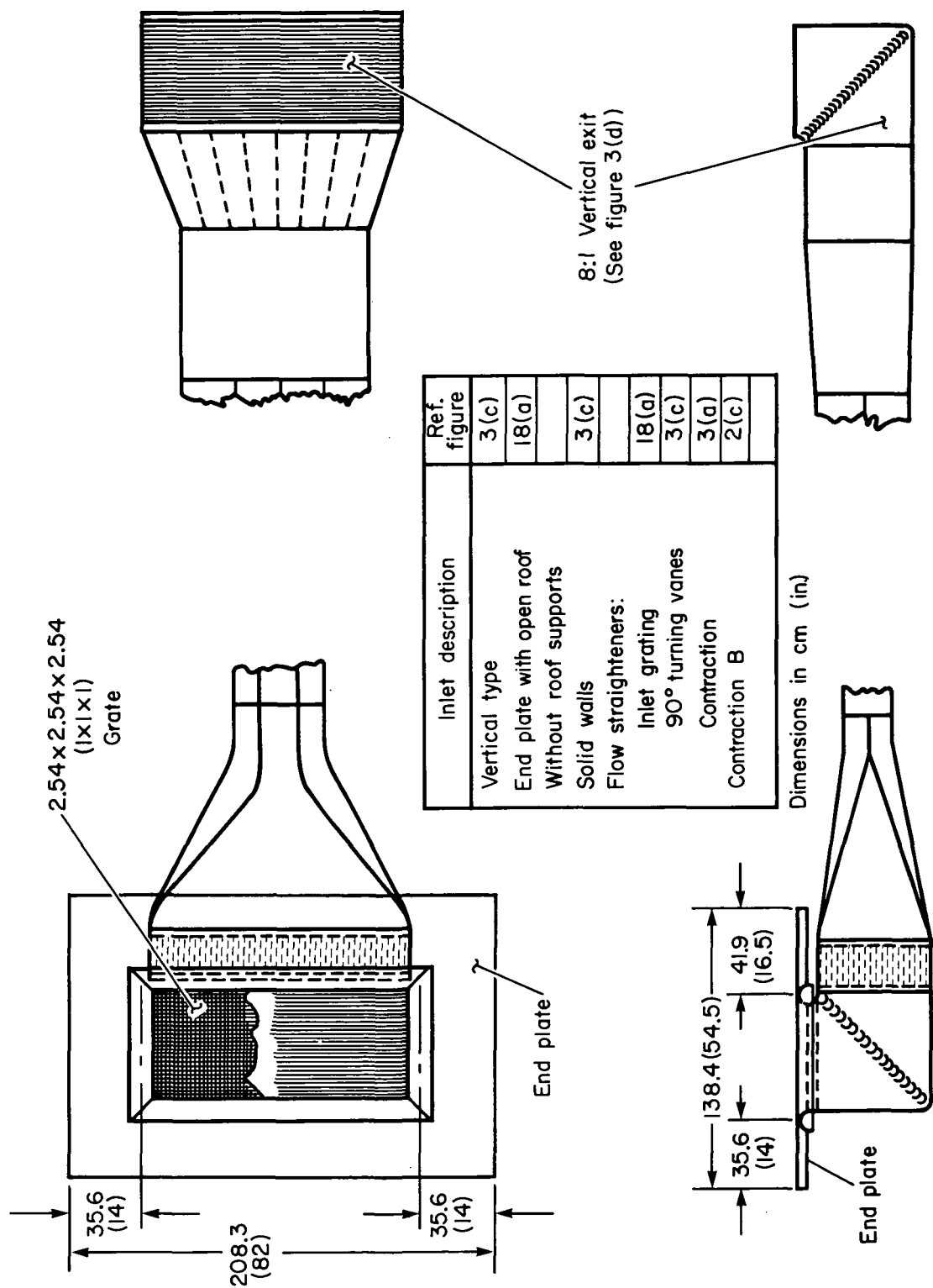
(a) End treatment configurations.

Figure 17.- Circuit with area-ratio-one horizontal inlet and 8:1 vertical exit.



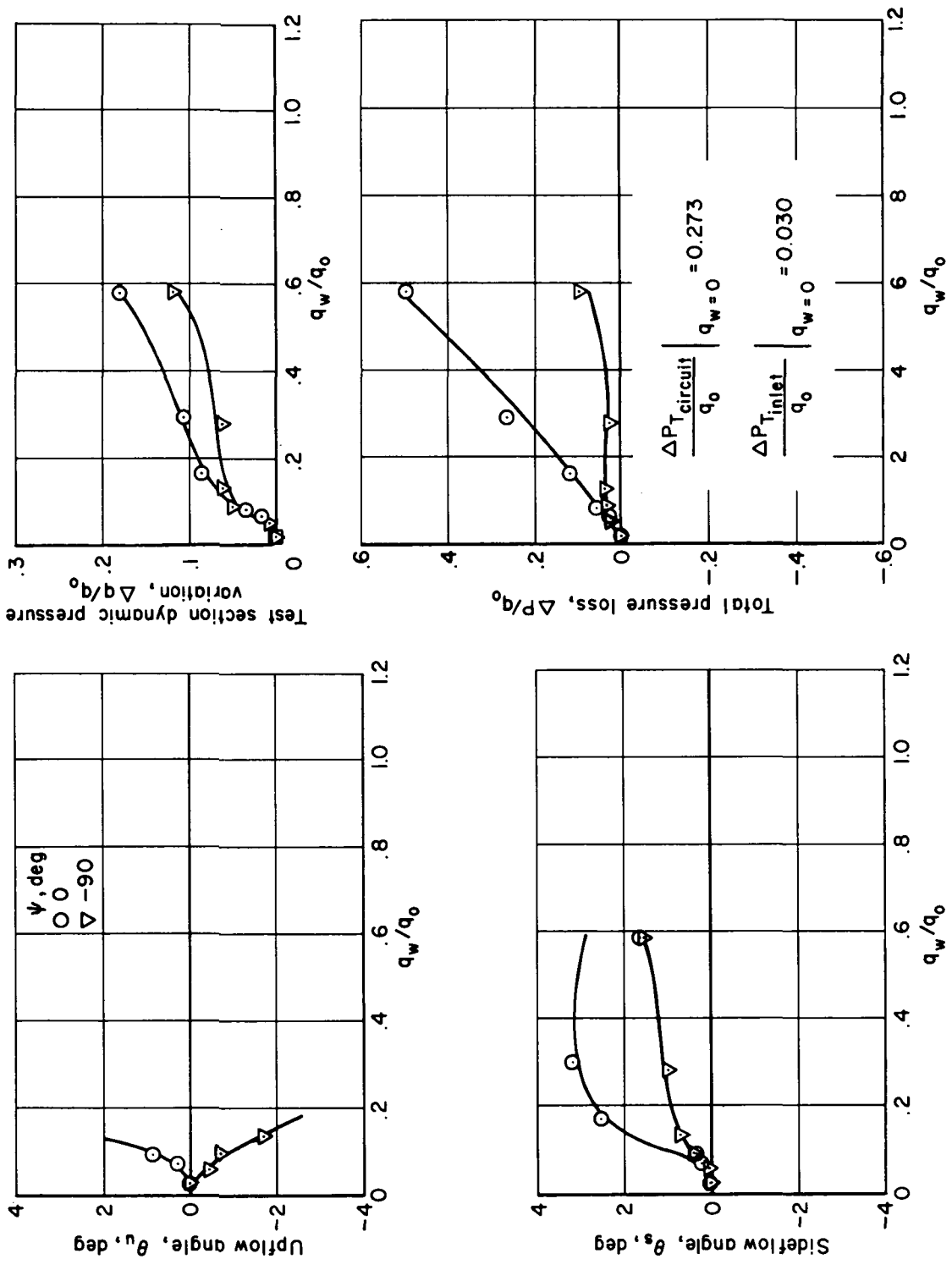
(b) Configuration flow results.

Figure 17.- Concluded.



(a) End treatment configurations.

Figure 18.- Circuit with 8:1 vertical inlet with grate, end plate, contraction flow straightener, and with 8:1 vertical exit.

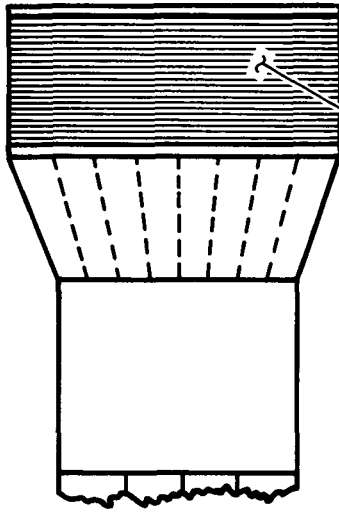
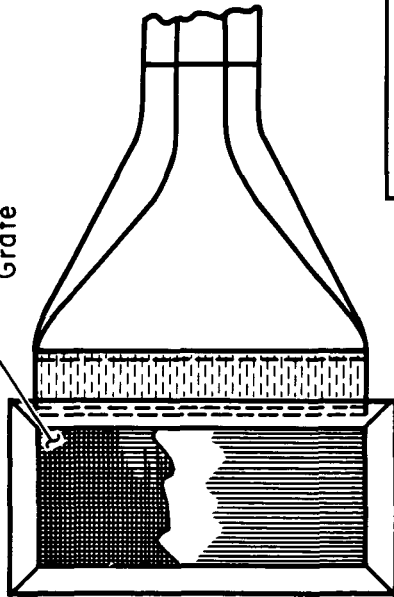


(b) Configuration flow results.

Figure 18.- Concluded.

2.54 x 2.54 x 2.54

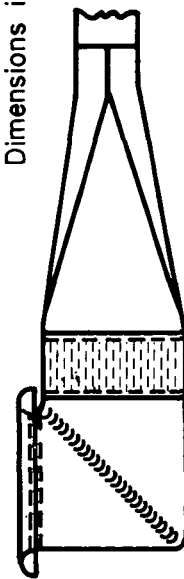
(1x1x1)
Grate



8:1 Vertical exit
(See figure 3(d))

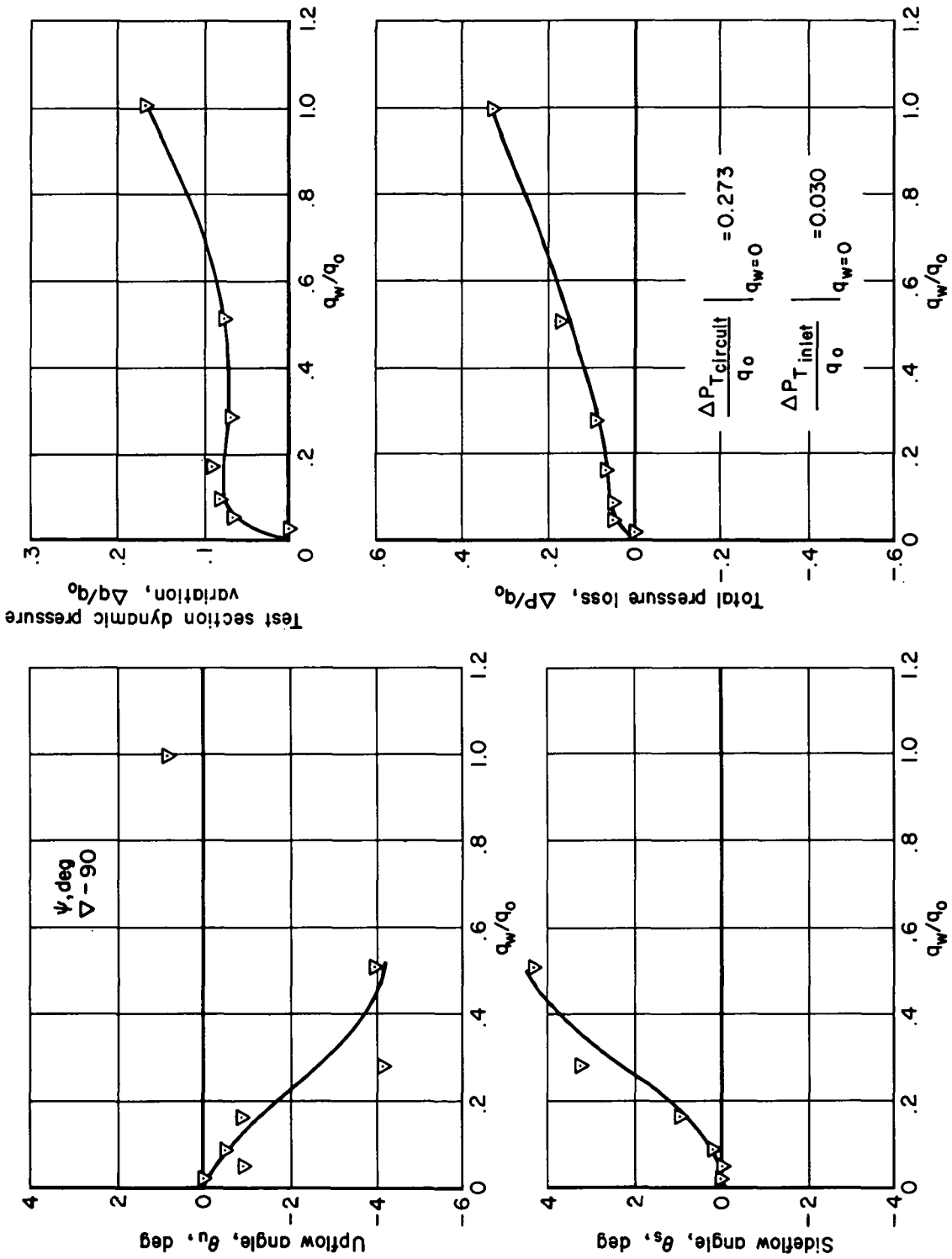
Inlet description	Ref. figure
Vertical type	3(c)
Without roof	
Without roof supports	
Solid walls	3(c)
Flow straighteners:	
Inlet grating	19(a)
90° turning vanes	3(c)
Contraction	3(a)
Contraction B	2(c)

Dimensions in cm (in.)



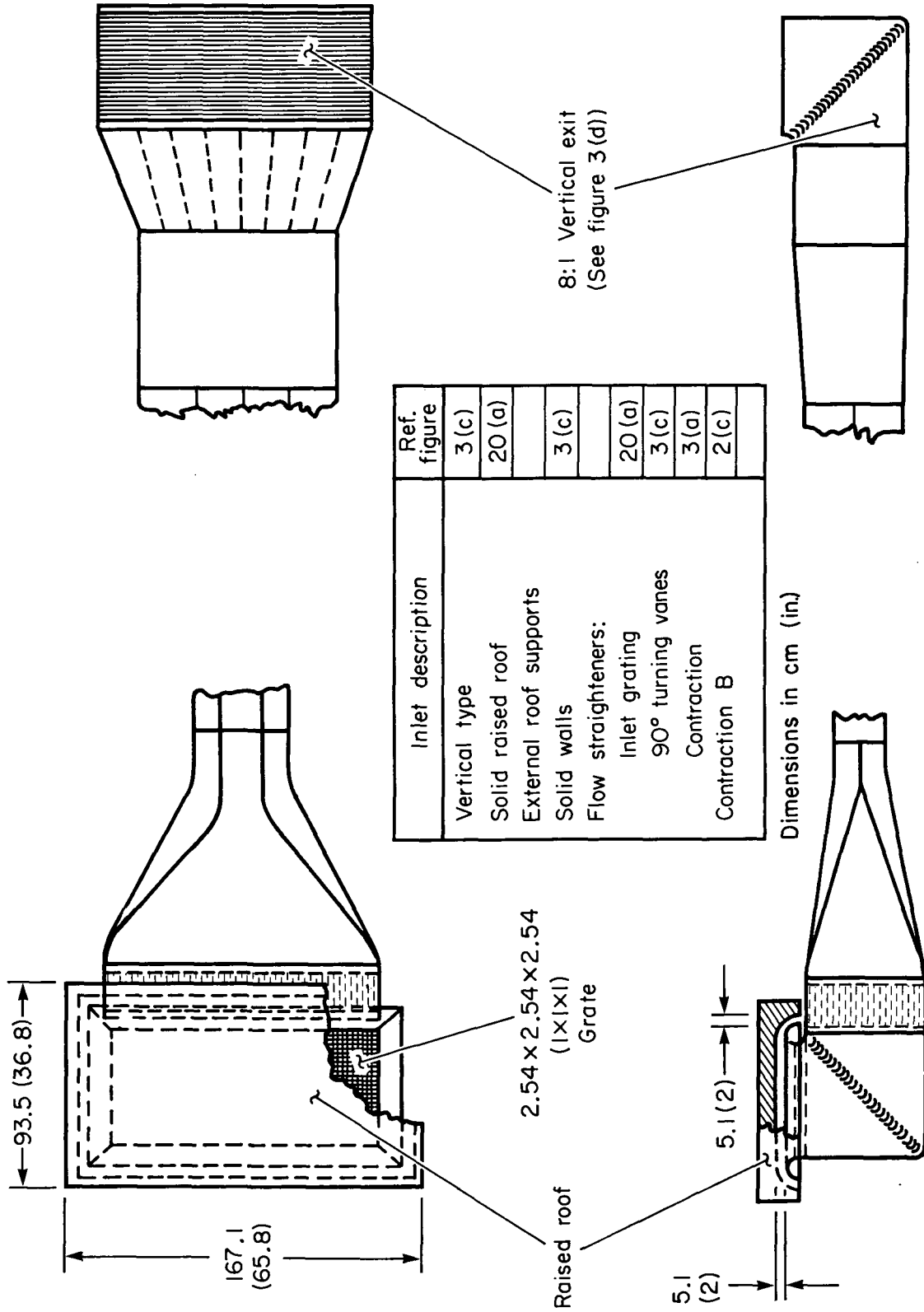
(a) End treatment configurations.

Figure 19.- Circuit with 8:1 vertical inlet with grate and 8:1 vertical exit.



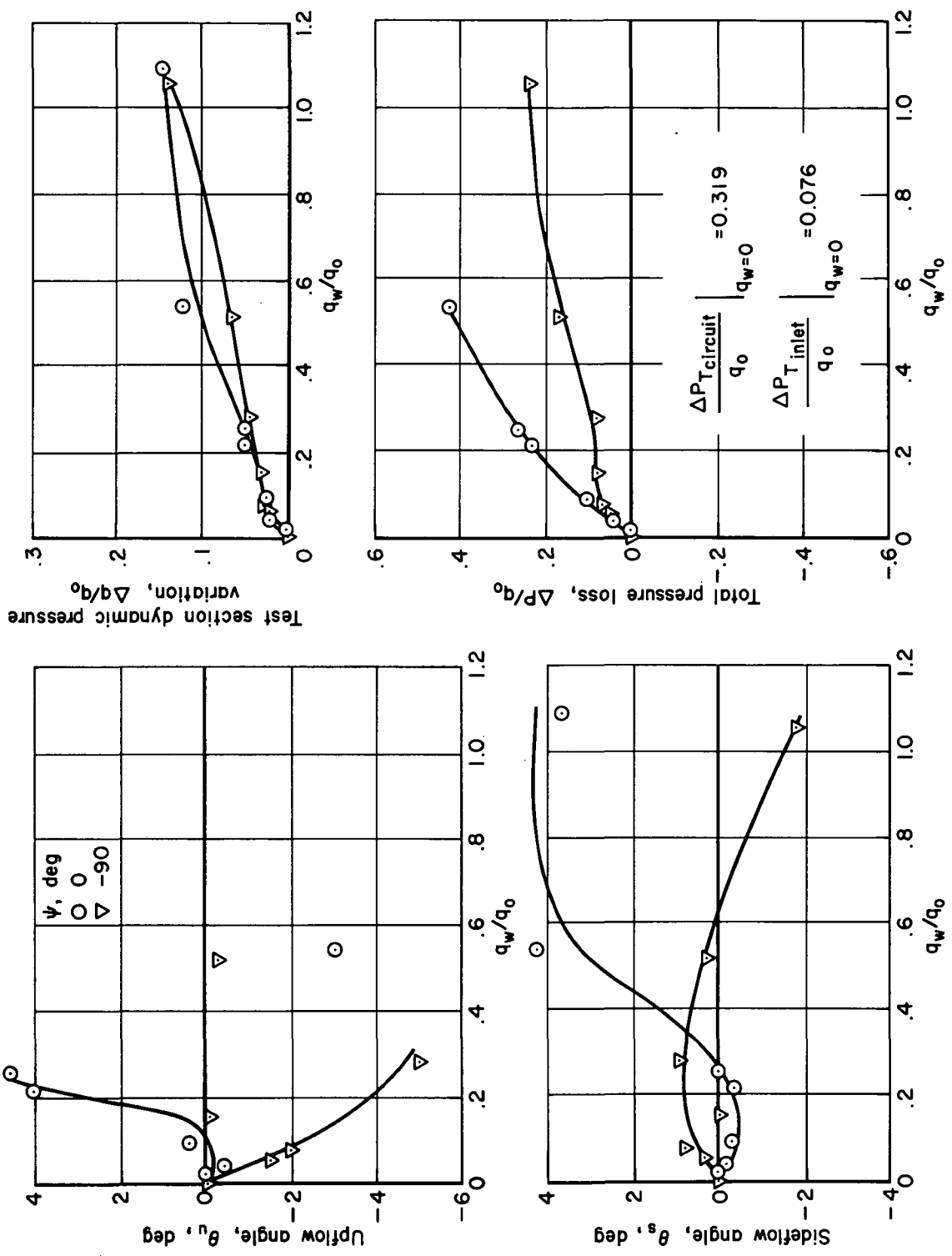
(b) Configuration flow results.

Figure 19.- Concluded.



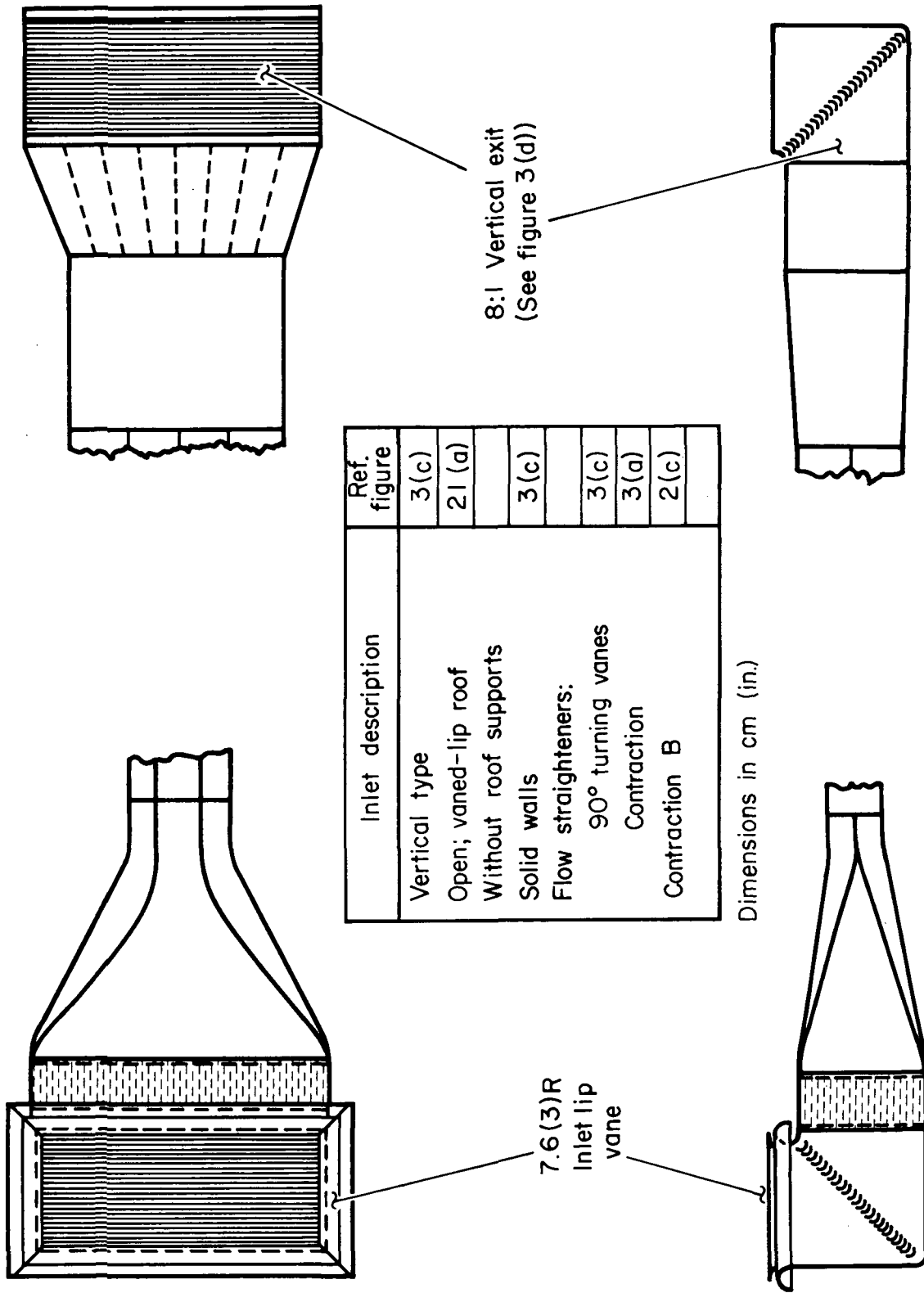
(a) End treatment configurations.

Figure 20.- Circuit with 8:1 vertical inlet with solid raised roof and 8:1 vertical exit.



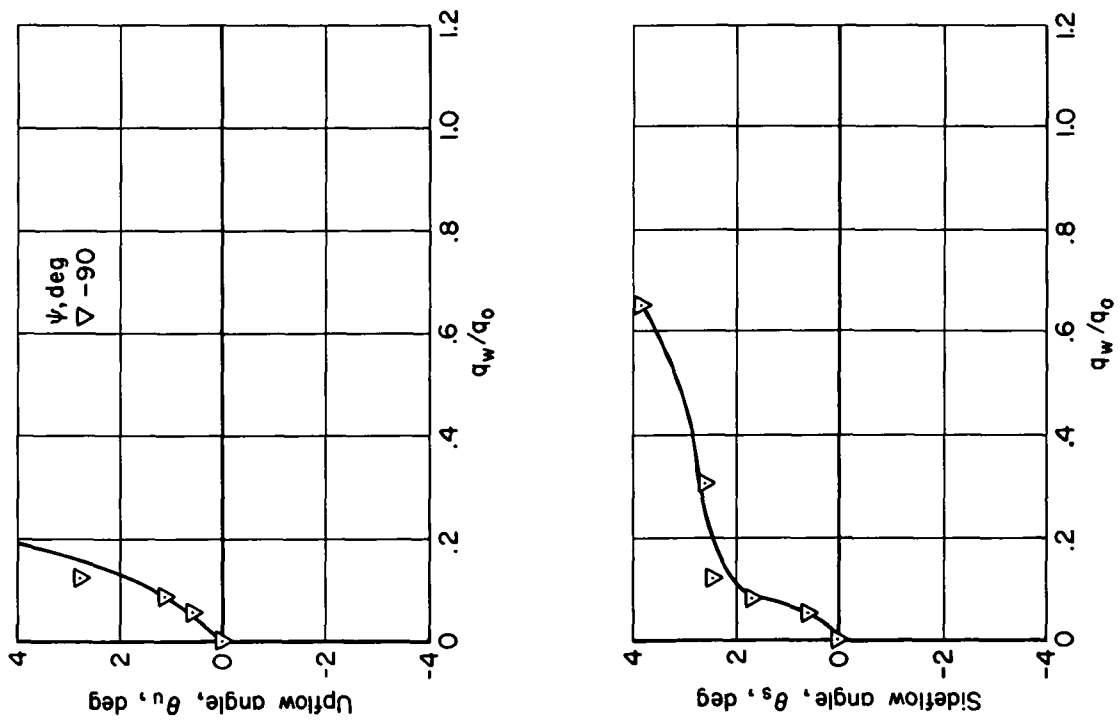
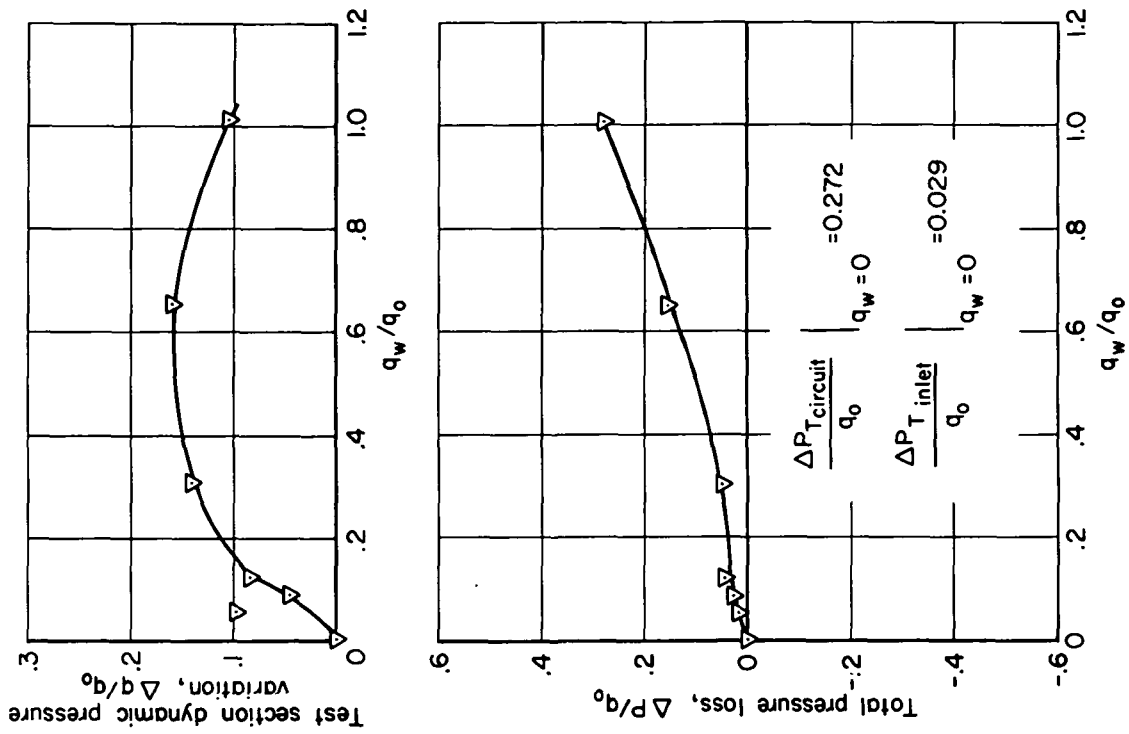
(b) Configuration flow results.

Figure 20.- Concluded.



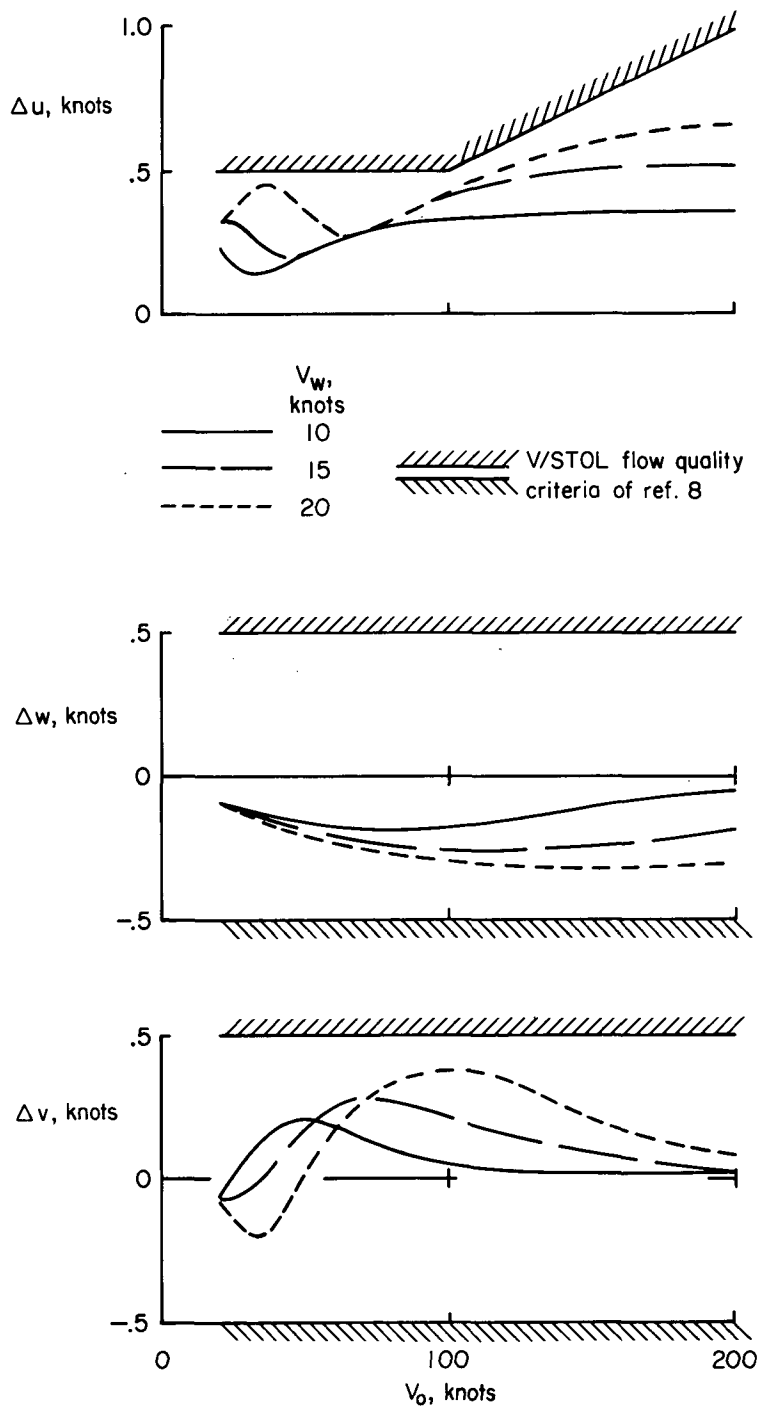
(a) End treatment configurations.

Figure 21.- Circuit with 8:1 vertical, vane inlet, and 8:1 vertical exit



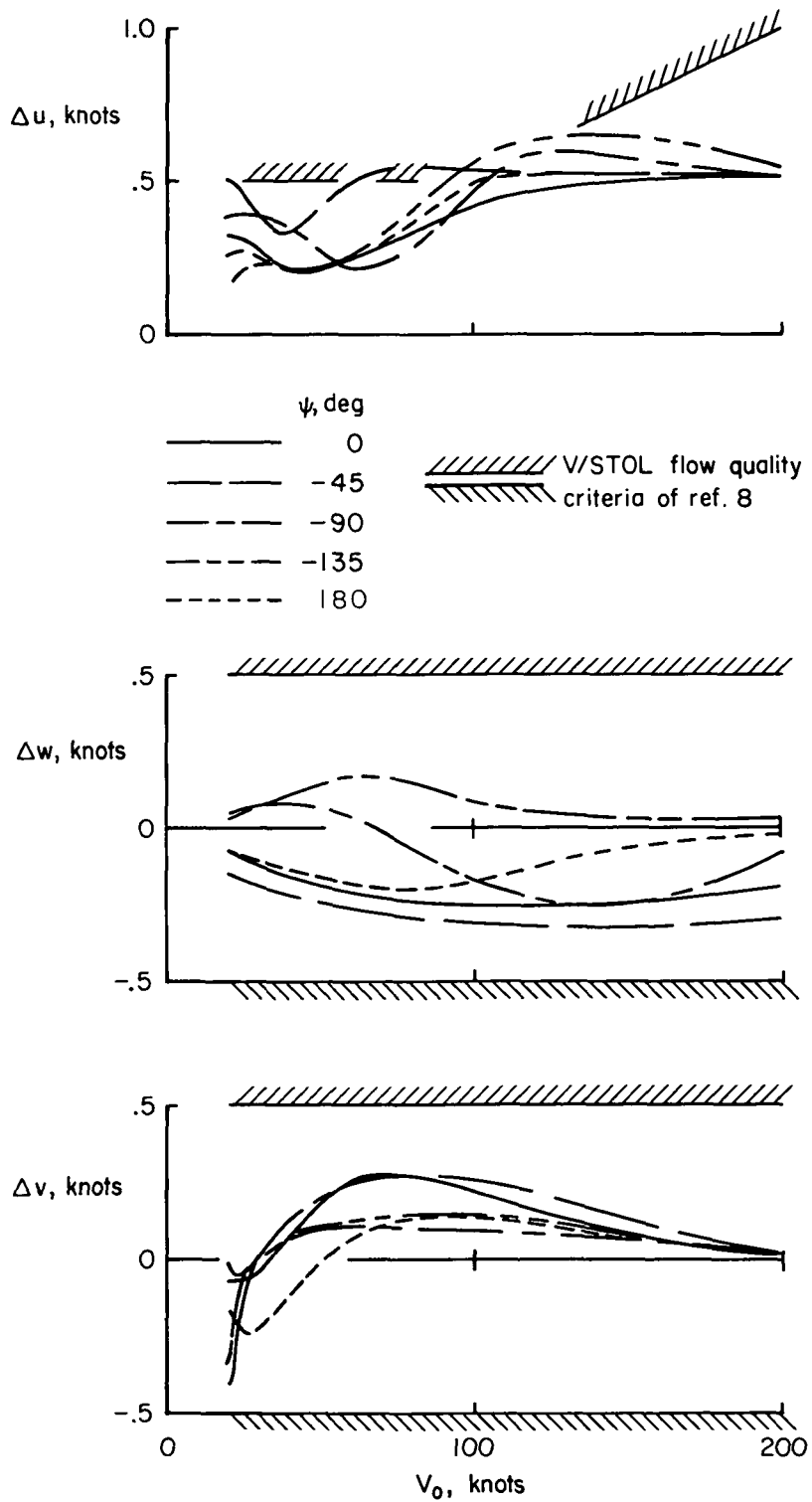
(b) Configuration flow results.

Figure 21.- Concluded.



(a) Effect of wind speed at $\Psi = 0^\circ$.

Figure 22.- Flow quality evaluation for model with 58 × 204 cm (23 × 80 in.) horizontal inlet with solid roof (post supports), 40 percent perforated-plate walls, peripheral flow straightener, 2.54 × 2.54 × 20.32 cm (1 × 1 × 8 in.) contraction flow straightener, and with 20:1 vertical exit - (configuration of figure 7).



(b) Effect of wind direction at $V_w = 15$ knots.

Figure 22.- Concluded.



POSTMASTER: If Undeliverable (Section 158
Postal Manual) Do Not Return

"The aeronautical and space activities of the United States shall be conducted so as to contribute . . . to the expansion of human knowledge of phenomena in the atmosphere and space. The Administration shall provide for the widest practicable and appropriate dissemination of information concerning its activities and the results thereof."

—NATIONAL AERONAUTICS AND SPACE ACT OF 1958

NASA SCIENTIFIC AND TECHNICAL PUBLICATIONS

TECHNICAL REPORTS: Scientific and technical information considered important, complete, and a lasting contribution to existing knowledge.

TECHNICAL NOTES: Information less broad in scope but nevertheless of importance as a contribution to existing knowledge.

TECHNICAL MEMORANDUMS: Information receiving limited distribution because of preliminary data, security classification, or other reasons. Also includes conference proceedings with either limited or unlimited distribution.

CONTRACTOR REPORTS: Scientific and technical information generated under a NASA contract or grant and considered an important contribution to existing knowledge.

TECHNICAL TRANSLATIONS: Information published in a foreign language considered to merit NASA distribution in English.

SPECIAL PUBLICATIONS: Information derived from or of value to NASA activities. Publications include final reports of major projects, monographs, data compilations, handbooks, sourcebooks, and special bibliographies.

TECHNOLOGY UTILIZATION PUBLICATIONS: Information on technology used by NASA that may be of particular interest in commercial and other non-aerospace applications. Publications include Tech Briefs, Technology Utilization Reports and Technology Surveys.

Details on the availability of these publications may be obtained from:

SCIENTIFIC AND TECHNICAL INFORMATION OFFICE

NATIONAL AERONAUTICS AND SPACE ADMINISTRATION
Washington, D.C. 20546